An Exactly Divergence-free Finite Element Method for Non-isothermal Flow Problems

by

Tong Qin

B.S. University of Science and Technology of China, 2011

A THESIS SUBMITTED IN PARTIAL FULFILLMENT OF

THE REQUIREMENTS FOR THE DEGREE OF

Master of Science

in

THE FACULTY OF GRADUATE AND POSTDOCTORAL STUDIES

(Mathematics)

The University of British Columbia

(Vancouver)

August 2013

Abstract

In this thesis the exactly divergence-free finite element method developed in [13] and [14] is studied. This method is first reviewed in the context of Stokes problem. An interior penalty discontinuous Galerkin approach is formulated and analysed in the framework of [13], [14] and [37]. Then we extend the method to non-isothermal flow problems, in particular, to a generalised Boussinesq equation. Following [34], the method is formulated and the numerical analysis is reviewed. Numerical examples are implemented and presented, which verify the theoretical error estimates and the exactly divergence-free property.

Preface

In this dissertation, the theoretical analysis in Chapter 1 is a review and synthesis of the work in [13], [14] and [37]. And the numerical experiments in Section 2.5 are carried out independently by the author T. Qin. The Chapter 2 is a summary and review of the paper [34] which is a collaboration with R. Oyarzúa and D. Schötzau. The formulation of the method is an extension of the work in [14]. The theoretical analysis is attributed to Oyarzúa and Schötzau. The author formulated the fixed-point iteration in Section 3.7 and extended the code to the generalized Boussinesq equation in Section 3.8. All the numerical experiments in this thesis are conducted with the *deal.II* finite element library [5]. A journal paper related with the work in Chapter 2 has been submitted to and accepted by the *IMA Journal of Applied Mathematics*.

Contents

List of Tables

List of Figures

Acknowledgements

First, I would like to express my sincere gratitude to my supervisor, Prof. Dominik Schötzau, for his thoughtful guidance, consistent encouragement and patient discussion throughout my graduate study and the writing of this thesis. I could not have imagined having a better advisor and mentor for my master's study.

I would also like to express my gratitude to my friends, office mates and room mates. They not only bring me help in both work and life but also make my life colourful. Special thanks to my girlfriend Yang Chen, without whose love and insistence, I could not get this far.

Last but not least, I want to express my sincere appreciation to all the helpful staff of the Mathematics Department and the Institute of Applied Mathematics at UBC, for providing excellent seminars and talks to enjoy and for providing a comfortable environment to work in. They really make me feel like a member of a big family!

Tong Qin

The University of British Columbia
August 2013

Chapter 1

Introduction

When simulating incompressible flow with finite element methods, the exact satisfaction of the incompressibility constraint $\nabla \cdot \mathbf{u} = 0$ is highly desirable. It yields provable energy-stable methods without the need to modify nonlinear terms in the underlying differential equations as is done in the classical methods for the incompressible Navier-Stokes equations in [40] and [41]. In contrast, failure to satisfy the constraint exactly can cause undesired instabilities especially in nonlinear problems, for example in collision flows in cross-shaped domains [32], and in the context of rotation-free forces acting on elastic materials [4]. In recent decades, many efforts have been made in designing efficient methods that are exactly divergence-free for incompressible flow problems in both conforming and the nonconforming setting. We mention here only [39, 42, 9, 22] and the references therein. In particular, in 2007, Cockburn, Kanschat and Schötzau developed and analysed a new exactly divergence-free element method for the incompressible Navier-Stokes problem, which is based on using divergence-conforming elements for the velocities and discontinuous elements for the pressure. The local approximation space pair $\mathbf{V} \times Q$ is chosen to satisfy the inclusion $\nabla \cdot \mathbf{V} \subseteq Q$. As shown in [14] and motivated by [13], this method is proved to be energy-stable, optimally convergent, locally conservative and yields exactly divergence-free velocity approximations. In [21], this method was further extended to an incompressible magnetohydrodynamics problem. In the first part of this thesis, this method is reviewed in the context of the analysis of the Stokes problem for quadrilateral meshes. Specifically, we follow [14] and employ the interior penalty discontinuous Galerkin (IPDG) method [1] to enforce the H^1-conformity of the velocity field. The local approximation space pair for the velocity and pressure is chosen to be the Raviart-Thomas element and the tensor product polynomial spaces (these are defined in Section 2.2) respectively, with equal approximation order k. The *a priori* error estimate is reviewed under the framework of [37] and is tested by numerical experiments.

The second part is devoted to extending this exactly divergence-free method to non-

isothermal flow problems. The simulation of non-isothermal flows is receiving more and more attention in many scientific and engineering branches such as the simulation of the convection process of the mantle in geophysical studies [29], the simulation of cooling processes in the device design and that of the polymer melting processes in industrial practice [26, 30], to name a few. Due to the importance of the model, numerical methods for this type of problem have been actively developed, see [15, 19, 17, 18] and the references therein. But none of them share the property of being exactly divergence-free in contrast to the method under consideration. In the second part of this thesis, we follow the work in [34] and consider the generalised Boussinesq equation, which couples the steady incompressible Navier-Stokes equation and a convection-diffusion equation through a nonlinear temperature-dependent viscosity and through a buoyancy term acting in the opposite direction of the gravity. The nonlinearity is addressed with a fixed-point approach. We extend the IPDG method from the first part as well as follow the work in [14] to discretize the linearized incompressible Navier-Stokes equation in each iteration. For the convection-diffusion equation, the standard conforming method is employed. The crucial aspect in the theoretical analysis is the construction of a suitable lifting of the temperature boundary data into the computational domain. A more restrictive assumption has to be made on the size of the solution. In the end of both parts, numerical experiments are conducted with the *deal.II* finite element library with the goal of verifying theoretical error estimates and the exactly divergence-free property.

Chapter 2

Divergence-Free Elements for the Stokes Problem

2.1 Introduction

In this chapter we recall and review the exactly divergence-free elements developed in [13] and [14] for the Stokes problem of incompressible fluid flow:

$$-\nu\Delta\mathbf{u} + \nabla p = \mathbf{f}, \qquad \text{in } \Omega \tag{2.1a}$$

$$\nabla \cdot \mathbf{u} = 0, \qquad \text{in } \Omega \tag{2.1b}$$

$$\mathbf{u} = \mathbf{g}, \qquad \text{on } \Gamma = \partial\Omega, \tag{2.1c}$$

where Ω is the computational domain in $\mathbb{R}^2$ and $\nu > 0$ denotes the kinematic viscosity, $\mathbf{u}$ the velocity, p the pressure and $\mathbf{f} \in (L^2(\Omega))^2$ the unit external volumetric force acting on the fluid. Furthermore the boundary datum $\mathbf{g} \in H^{1/2}(\Gamma)^2$ satisfies the compatibility condition:

$$\int_\Gamma \mathbf{g} \cdot \mathbf{n}\, ds = 0. \tag{2.2}$$

The exact satisfaction of the divergence constraint (2.1b) is a highly desirable property in the simulation of incompressible flows. It yields energy-stable methods without the need to modify nonlinear terms in the underlying differential equations as is done in the context of the incompressible Navier-Stokes equations in [40] and [41]. Not enforcing this constraint exactly may result in instabilities when simulating the incompressible steady flow problems, especially when a rotation-free part occurs in the external force vector or in a nonlinear convection term; see [32]. However, most of the stable finite element pairs, such as the Taylor-Hood element [24] and the MINI element [2] do not satisfy the divergence constraint exactly.

In the context of conforming finite element methods, in 1985, Scott and Vogelius [39] constructed inf-sup stable and exact divergence-free pairs by using continuous $\mathbb{P}_k$ elements, which are polynomials of maximal degree k, for the approximation of the velocity and the discontinuous $\mathbb{P}_{k-1}$ elements for the pressure. This pair is also employed in [32] as a comparison with the Taylor-Hood element to illustrate the importance of mass conservation in incompressible fluid simulation. Since $\nabla \cdot \mathbf{V}_h \subseteq Q_h$, it is obvious to see the exact divergence-free property. But this pair is proved to be stable on triangular grids without singular vertices with the polynomial degree satisfying $k \geq 4$. For smaller k, the meshes need to be Hsieh-Clough-Tocher or Powell-Sabin triangulations; see the review paper by Zhang [42]. Recently, Guzmán and Neilan overcame this difficulty and constructed finite element pairs for the Stokes problem on *general triangular meshes* that are inf-sup stable, optimally convergent and divergence-free; see [22] for 2D and [23] for 3D. The idea is to enrich the $H(\mathrm{div};\Omega)$-conforming elements locally with *divergence-free rational shape-functions*. These additional functions will help to enforce the continuity. For approaches with exactly divergence-free velocity approximation in the isogeometric analysis we refer to [9] which is based on a B-spline generalization of the Raviart-Thomas elements and to [4] for the application in the context of elasticity of nearly incompressible materials.

In this chapter, we will use a discontinuous Galerkin approach to exactly enforce the constraint (2.1b). This approach for Navier-Stokes equations was first introduced in [13] and [14] in the context of local discontinuous Galerkin (LDG) methods. The resulting methods are locally conservative, energy-stable, optimally convergent and exactly divergence-free. As pointed in [13], we adopt here the interior penalty approach for the viscous term. In this chapter, we review the formulation and analysis of this method by solving the model Stokes problem with Raviart-Thomas elements of order k for the velocity approximation and tensor product polynomials of degree k for the pressure.

2.2 Preliminaries and Notations

In order to formulate and analyse the DG methods, we introduce the following notations that will be used throughout this thesis.

Let Ω denote a polygonal domain in $\mathbb{R}^2$ with Lipschitz boundary $\Gamma = \partial\Omega$. Suppose we have a quasi-uniform and regular (see [11]) triangulation $\mathcal{T}_h$ of the domain Ω into elements $\{K\}$. We denote the elemental diameter by h_K and, as usual, define the meshsize $h = \max_{K\in\mathcal{T}_h} h_K$. We further denote by $\mathcal{E}_h^{\mathcal{I}}$ the set of all interior edges of $\mathcal{T}_h$ and by $\mathcal{E}_h^{\mathcal{B}}$ the set of all boundary edges. We set $\mathcal{E}_h = \mathcal{E}_h^{\mathcal{I}} \cup \mathcal{E}_h^{\mathcal{B}}$.

The standard definitions are used for the Lebesgue and Sobolev spaces $L^p(\Omega)$ and $W^{r,p}(\Omega)$, where $r \geq 0$ and $p \in [1, \infty]$, with the norms $\|\cdot\|_{L^p(\Omega)}$ and $\|\cdot\|_{W^{r,p}(\Omega)}$, respectively. We write $H^r(\Omega)$ instead of $W^{r,2}(\Omega)$ and denote the associated seminorms by $|\cdot|_{r,\Omega}$. For vector-valued function, we denote $\mathbf{H}^r(\Omega) = H^r(\Omega)^2$ and $\mathbf{L}^r(\Omega) = L^r(\Omega)^2$. Moreover, we will use the vector-valued Hilbert spaces

$$H(\mathrm{div}; \Omega) = \{\mathbf{v} \in (\mathrm{L}^2(\Omega))^2, \nabla \cdot \mathbf{v} \in \mathrm{L}^2(\Omega)\}$$

with the norm

$$\|\mathbf{v}\|^2_{\mathrm{div},\Omega} = \|\mathbf{v}\|^2_{0,\Omega} + \|\nabla \cdot \mathbf{v}\|^2_{0,\Omega}$$

On the reference element $\hat{K}$, for nonnegative integers k and l, the spaces $\mathbb{Q}_{k,l}(\hat{K})$ consist of polynomials of degree at most k and l in the first and second variables, respectively. When $k = l$, the notation $\mathbb{Q}_k(\hat{K})$ is adopted instead of $\mathbb{Q}_{k,k}(\hat{K})$. And we use $\mathbb{P}_k(K)$ and $\mathbb{P}_k(e)$ to denote the space of polynomials of maximal degree k defined in any element K and any edge e, respectively. We assume that each element $K \in \mathcal{T}_h$ is the image of the reference element $\hat{K} = (-1, 1)^2$ under the invertible affine mapping $F_K : \hat{K} \to K$, with $F_K(\hat{\mathbf{x}}) = B_K\hat{\mathbf{x}} + \mathbf{b}_K$, $B_K \in \mathbb{R}^{2\times 2}$, $\mathbf{b}_K \in \mathbb{R}^2$.

To define the DG method, we introduce notations associated with traces. Let K^+ and K^- be two adjacent elements of $\mathcal{T}_h$. Let $\mathbf{x}$ be an arbitrary point of the interior edge $e = \partial K^+ \cap \partial K^- \in \mathcal{E}_h^{\mathcal{I}}$. Let ϕ be a piecewise smooth scalar-, vector-, or matrix-valued function and let us denote by $\phi^{\pm}$ the traces of ϕ on e taken from within the interior of $K^{\pm}$. Then, we define the mean value $\{\!\{\cdot\}\!\}$ at $\mathbf{x} \in e$ as

$$\{\!\{\phi\}\!\} := \frac{1}{2}(\phi^+ + \phi^-).$$

where ϕ can be any piecewise smooth scalar-, vector- or tensor-valued function. Further, we define the jumps $[\![\cdot]\!]$ at $\mathbf{x} \in e$ as

for $e \in \mathcal{E}_h^I$:

$$[\![q]\!] := (q^+ - q^-)\mathbf{n}_{K^+}, \quad \underline{[\![\mathbf{v}]\!]} := (\mathbf{v}^+ - \mathbf{v}^-) \otimes \mathbf{n}_{K^+}, \quad [\![\mathbf{v}]\!] := (\mathbf{v}^+ - \mathbf{v}^-) \cdot \mathbf{n}_{K^+},$$

for $e \in \mathcal{E}_h^B$:

$$[\![q]\!] := q\mathbf{n}, \quad \underline{[\![\mathbf{v}]\!]} := \mathbf{v} \otimes \mathbf{n}, \quad [\![\mathbf{v}]\!] := \mathbf{v} \cdot \mathbf{n},$$

Here, q is any scalar-valued function, $\mathbf{v}$ is a vector-valued one and $\mathbf{n}_K$ denotes an outward unit normal vector on the boundary ∂K of element K and $(\mathbf{v} \otimes \mathbf{n})_{ij} = v_i n_j$.

We end this section by a summation identity from [3], which will be used to transform the local formulation the DG methods to the global one:

$$\sum_{K\in\mathcal{T}_h}\int_{\partial K} q\mathbf{v}\cdot\mathbf{n}\,ds = \int_{\mathcal{E}_h}\{\!\{\mathbf{v}\}\!\}\cdot[\![q]\!]\;ds + \int_{\mathcal{E}_h^I}\{\!\{q\}\!\}\,[\![\mathbf{v}]\!]\;ds \tag{2.3}$$

2.3 Divergence-Free Elements for the Stokes Problem

2.3.1 The Stokes Problem

For simplicity and without loss of generality, from this section on, we take $\nu = 1$. We introduce the solution spaces $\mathbf{V}$ and Q which are defined to be

$$\mathbf{V} = \mathbf{H}^1(\Omega), \qquad Q = L_0^2(\Omega) = \left\{ q \in L^2(\Omega) : \int_\Omega q\,d\mathbf{x} = 0 \right\} \tag{2.4}$$

The weak formulation of (2.1) is to find $(\mathbf{u}, p) \in \mathbf{V}\times Q$ with $\mathbf{u}|_\Gamma = \mathbf{g}$ such that

$$\left\{ \begin{array}{rcl} A(\mathbf{u},\mathbf{v}) + B(\mathbf{v},q) &=& (\mathbf{f},\mathbf{v}) \\ B(\mathbf{u},q) &=& 0 \end{array} \right. \tag{2.5}$$

for all $(\mathbf{v}, q) \in \mathbf{H}_0^1(\Omega)\times L_0^2(\Omega)$ where the bilinear forms $A(\cdot,\cdot)$ and $B(\cdot,\cdot)$ are defined as

$$A(\mathbf{u},\mathbf{v}) = \int_\Omega \nabla\mathbf{u} : \nabla\mathbf{v}\,d\mathbf{x}, \qquad B(\mathbf{u},p) = -\int_\Omega p\nabla\cdot\mathbf{u}d\mathbf{x} \tag{2.6}$$

The well-posedness of (2.5) is ensured by the continuity of $A(\cdot,\cdot)$ and $B(\cdot,\cdot)$, the coercivity of $A(\cdot,\cdot)$, and the following inf-sup condition

$$\inf_{0\neq q\in L_0^2(\Omega)}\sup_{\mathbf{0}\neq\mathbf{v}\in H_0^1(\Omega)^d} \frac{-\int_\Omega q\nabla\cdot\mathbf{v}}{|\mathbf{v}|_1\|q\|_0} \geq \gamma > 0 \tag{2.7}$$

with an inf-sup constant γ only depending on Ω; see [8].

2.3.2 Discrete Spaces

We will use the following discrete spaces when formulating the DG method.

$$\mathbf{U}_h = \{\mathbf{v}\in L^2(\Omega)^2 : \mathbf{v}|_K \in \mathbb{Q}_{k+1}(K),\ K\in\mathcal{T}_h\} \tag{2.8}$$

$$\mathbf{V}_h = \{\mathbf{v}\in H(\mathrm{div};\Omega) : \mathbf{v}|_{\mathrm{K}} \in \mathbf{RT}_{\mathrm{k}}(\mathrm{K}),\ \mathrm{K}\in\mathcal{T}_{\mathrm{h}};\ \mathbf{v}\cdot\mathbf{n} = \mathrm{g_h}\ \mathrm{on}\ \Gamma\} \tag{2.9}$$

$$\mathbf{V}_h^0 = \{\mathbf{v}\in H(\mathrm{div};\Omega) : \mathbf{v}|_{\mathrm{K}} \in \mathbf{RT}_{\mathrm{k}}(\mathrm{K}),\ \mathrm{K}\in\mathcal{T}_{\mathrm{h}};\ \mathbf{v}\cdot\mathbf{n} = 0\ \mathrm{on}\ \Gamma\} \tag{2.10}$$

$$Q_h = \{q\in Q : q\in\mathbb{Q}_k(K),\ K\in\mathcal{T}_h\} \tag{2.11}$$

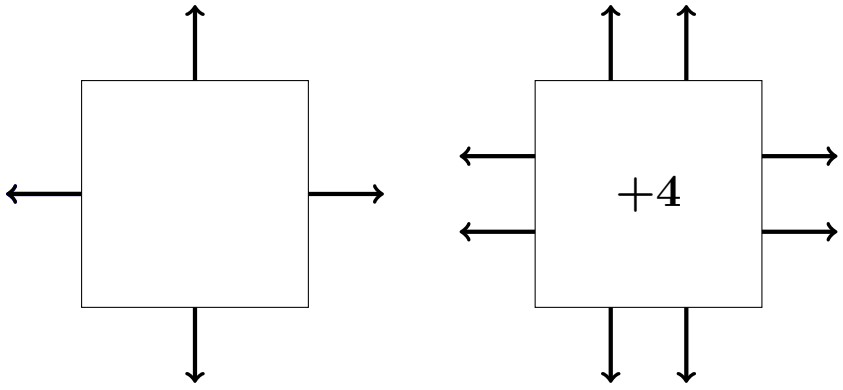

Figure 2.1: The illustration for the distribution of dofs of the $\mathbf{RT}_0$ (left) and $\mathbf{RT}_1$ (right) elements

where g_h is the L^2 projection of $\mathbf{g} \cdot \mathbf{n}$ into the space $\mathbb{P}_k(e)$, or equivalently,

$$\int_e \mathbf{g} \cdot \mathbf{n} \phi \, ds = \int_e g_h \phi \, ds, \quad \forall \phi \in \mathbb{P}_k(e), \, \forall e \in \mathcal{E}_h^B \tag{2.12}$$

We will see the reason for this definition in following sections, especially in the proofs of Proposition 2.3.3 (the divergence-free property) and Theorem 2.4.7 (the *a priori* error estimate).

On the reference element $\hat{K} = (-1, 1)^2$, the Raviart-Thomas space of order k ($\mathbf{RT}_k$) is defined (see [8, Section 3.2]) by

$$\mathbf{RT}_k(\hat{K}) = \mathbb{Q}_{k+1,k}(\hat{K}) \times \mathbb{Q}_{k,k+1}(\hat{K})$$

with the corresponding interpolation operator $\widehat{\mathbf{\Pi}}_k$ satisfying $\widehat{\mathbf{\Pi}}_k \mathbf{u} \in \mathbf{RT}_k$ and

$$\begin{cases} \int_{\hat{K}} (\widehat{\mathbf{\Pi}}_k \hat{\mathbf{u}} - \hat{\mathbf{u}}) \cdot \hat{\mathbf{v}} = 0, & \forall \hat{\mathbf{v}} \in \mathbb{Q}_{k-1,k}(\hat{K}) \times \mathbb{Q}_{k,k-1}(\hat{K}) \\ \int_{\gamma_m} (\widehat{\mathbf{\Pi}}_k \hat{\mathbf{u}} - \hat{\mathbf{u}}) \cdot \hat{\mathbf{n}} \, \hat{q} \, d\hat{s} = 0, & \forall \hat{q} \in \mathbb{P}_k(\gamma_m), \quad m = 1, ..., 4 \end{cases} \tag{2.13}$$

where γ_m, $m = 1, ..., 4$ are the boundary edges of $\hat{K}$. In Figure 2.1, we take the $\mathbf{RT}_0(\hat{K})$ and $\mathbf{RT}_1(\hat{K})$ elements as examples to illustrate the distribution of the degrees of freedom (dofs) of the Raviart-Thomas element. The arrows on the boundary represent the dofs related with the normal component. And the number in the cell is the number of dofs located inside the cell.

On a general physical element K, it's easy to check that the affine transformation F_K

does not preserve the degrees of freedom $\int_{\gamma_m} \mathbf{u}\cdot\mathbf{n}\, q\, ds$, for $q \in \mathbb{P}_k(\gamma_m)$. The Piola transformation, which is defined as

$$\mathcal{P}_K \hat{\mathbf{u}} = \frac{1}{\det \mathbf{B}_K} \mathbf{B}_K \hat{\mathbf{u}} \circ F_K^{-1}, \tag{2.14}$$

overcomes this difficulty. It was first introduced in the continuum mechanics to map vectors between Eulerian and Lagrangian coordinates while preserving the total flux over the boundary, i.e., $\int_{\partial \hat{G}} \hat{\mathbf{v}}\cdot\hat{\mathbf{n}}\, d\hat{s} = \int_{\partial G} \mathbf{v}\cdot\mathbf{n}\, ds$, where $\hat{G}$ is a reference volume (Lagrangian coordinate) and G is the deformed one (Eulerian coordinate); see [12].

In general, we have following properties of the Piola transformation.

Lemma 2.3.1 *For $q \in H^1(\hat{K})$, $\hat{\mathbf{v}} \in H(\widehat{\mathrm{div}}, \hat{K})$ and $q := \hat{q}\circ F_K^{-1}$, $\mathbf{v} = \mathcal{P}(\hat{\mathbf{v}})$, the Piola transformation preserves the following quantities:*

$$\int_K \mathbf{v}\cdot\nabla q\, d\mathbf{x} = \int_{\hat{K}} \hat{\mathbf{v}}\cdot\hat{\nabla}\hat{q}\, d\hat{\mathbf{x}}, \tag{2.15}$$

$$\int_K \nabla\cdot\mathbf{v}\, q\, d\mathbf{x} = \int_{\hat{K}} \hat{\nabla}\cdot\hat{\mathbf{v}}\hat{q}\, d\hat{\mathbf{x}} \tag{2.16}$$

$$\int_{\partial K} \mathbf{v}\cdot\mathbf{n}\, q\, ds = \int_{\partial \hat{K}} \hat{\mathbf{v}}\cdot\hat{\mathbf{n}}\hat{q}\, d\hat{s} \tag{2.17}$$

■

Proof: For the affine transformation, the proof is very simple. We add it here for completeness. An application of the chain rule gives the following result

$$\nabla = \mathbf{B}_K^{-T}\hat{\nabla} \tag{2.18}$$

Then we have

$$\begin{aligned}\int_K \mathbf{v}\cdot\nabla q\, d\mathbf{x} &= \int_{\hat{K}} \left(\frac{1}{\mathrm{det}\mathbf{B}_\mathrm{K}}\mathbf{B}_K\hat{\mathbf{u}}\right)\cdot(\mathbf{B}_K^{-T}\hat{\nabla}\hat{q})\,\mathrm{det}\mathbf{B}_\mathrm{K}\,\mathrm{d}\hat{\mathbf{x}}\\ &= \int_{\hat{K}} (\mathbf{B_K}^{-1}\mathbf{B}_K) : \hat{\mathbf{u}}\otimes\hat{\nabla}\hat{q}\, d\hat{\mathbf{x}}\\ &= \int_{\hat{K}} \hat{\mathbf{u}}\cdot\hat{\nabla}\hat{q}\, d\hat{\mathbf{x}}.\end{aligned}$$

For the equation (2.16), first, we notice that

$$\begin{aligned}\nabla\mathbf{v} &= \mathbf{B}_K^{-T}\hat{\nabla}\left(\frac{1}{\mathrm{det}\mathbf{B}_\mathrm{K}}\mathbf{B}_K\hat{\mathbf{v}}\right)\\ &= \frac{1}{\mathrm{det}\mathbf{B}_\mathrm{K}}\mathbf{B}_K^{-T}\hat{\nabla}\hat{\mathbf{v}}\mathbf{B}_K^T.\end{aligned}$$

Since the trace is invariant under a similarity transformation, we further have

$$\nabla \cdot \mathbf{v} = \frac{1}{\det \mathbf{B}_{\mathrm{K}}} \hat{\nabla} \cdot \hat{\mathbf{v}}. \tag{2.19}$$

Then equation (2.16) follows by a simple substitution.
At last, it is easy to see that equation (2.17) can be obtained by divergence theorem and equations (2.15) and (2.16). ■

Remark From the proof above we see that in Piola transformation, the factor $\frac{1}{\det \mathbf{B}_{\mathrm{K}}}$ is introduced to cancel out the scaling factor. And the matrix $\mathbf{B}_K$ is for balancing the factor $\mathbf{B}_K^{-T}$ appearing in the gradient operator in (2.18).

From the last identity we see that the Piola transformation preserves the normal trances in $H^{-1/2}(\partial \hat{K})$, which makes it a suitable transformation for the $H(\mathrm{div})$ spaces. Therefore we can define the $\mathbf{RT}_k(K)$ space as $\mathcal{P}_K(\mathbf{RT}_k(\hat{K}))$. For more properties of both the $\mathbf{RT}_k$ element and the Piola transformation, one can refer to [8].

For nonnegative integer k, l, the tensor product polynomial spaces $\mathbb{Q}_{k,l}(K)$ on the physical element K are defined via the affine mapping F_K as

$$\mathbb{Q}_{k,l}(K) := \{q : \ q(x,y) = \hat{q} \circ F_K^{-1}(x,y), \ \hat{q} \in \mathbb{Q}_{k,l}(K)\} \tag{2.20}$$

and when $k = l$, we denote $\mathbb{Q}_k(K) = \mathbb{Q}_{k,k}(K)$. Then it is obvious to get $\mathbf{V}_h \subseteq \mathbf{U}_h$ and $\mathbf{V}_h^0 \subseteq \mathbf{U}_h$.

We end this section by an important relationship between $\mathbf{RT}_k(K)$ and $\mathbb{Q}_k(K)$, which, we will see, plays a key role in ensuring the exact divergence-free property.

Proposition 2.3.2 *For affine elements $K \in \mathcal{T}_h$, the local approximation space pair $\mathbf{RT}_k(K)$ and $\mathbb{Q}_k(K)$ satisfies the following inclusion:*

$$\nabla \cdot \mathbf{RT}_k(K) \subseteq \mathbb{Q}_k(K) \tag{2.21}$$

Proof: First on the reference element K, by the definition of $\mathbf{RT}_k(\hat{K})$ it is obvious to see that

$$\hat{\nabla} \cdot \mathbf{RT}_k(\hat{K}) = \mathbb{Q}_k(\hat{K}) \tag{2.22}$$

In the proof of the last proposition we have obtained

$$\nabla \cdot \mathbf{v} = \frac{1}{\det \mathbf{B}_{\mathrm{K}}} \hat{\nabla} \cdot \hat{\mathbf{v}}, \tag{2.23}$$

for $\mathbf{v} \in \mathbf{RT}_k(K)$. Due to (2.22), we know that there exists a polynomial $\hat{q} \in \mathbb{Q}_k(\hat{K})$ such that $\hat{\nabla} \cdot \hat{\mathbf{v}} = \hat{q}$. Then by the definition of $\mathbb{Q}_k(K)$, we have

$$\nabla \cdot \mathbf{v} = \frac{1}{\det \mathbf{B}_\mathrm{K}} \hat{q} \circ F_K^{-1} \in \mathbb{Q}_k(K)$$

which implies the conclusion. ■

2.3.3 Formulation of the interior penalty DG Method

We denote $(\mathbf{u}_h, p_h) \in \mathbf{V}_h \times Q_h$ to be the numerical approximation. First, we follow the procedure in [3] and discretize each component of the viscous term with the symmetric interior penalty method [1]. Then we get the elliptic form

$$\begin{aligned} A_h(\mathbf{u}_h, \mathbf{v}) = & \int_\Omega \nabla_h \mathbf{u}_h : \nabla_h \mathbf{v} d\mathbf{x} \\ & + \frac{\kappa_0}{h} \int_{\mathcal{E}_h^I} \underline{[\![\mathbf{u}_h]\!]} : \underline{[\![\mathbf{v}]\!]} \, ds - \int_{\mathcal{E}_h^I} \underline{[\![\mathbf{u}_h]\!]} : \{\!\{\nabla_h \mathbf{v}\}\!\} \, ds - \int_{\mathcal{E}_h^I} \underline{[\![\mathbf{v}]\!]} : \{\!\{\nabla_h \mathbf{u}_h\}\!\} \, ds \\ & + \frac{\kappa_0}{h} \int_{\mathcal{E}_h^B} \mathbf{u}_h \cdot \mathbf{v} \, ds - \int_{\mathcal{E}_h^B} (\mathbf{u}_h \otimes \mathbf{n}) : \nabla_h \mathbf{v} \, ds - \int_{\mathcal{E}_h^B} (\mathbf{v} \otimes \mathbf{n}) : \nabla_h \mathbf{u}_h \, ds \end{aligned} \quad (2.24)$$

for $\mathbf{v}$ in $\mathbf{V}_h^0$. The penalty parameter κ_0 is chosen sufficiently large but independent of h. The broken gradient operator ∇_h is defined as $\nabla_h \mathbf{v}|_K = \nabla \mathbf{v}$.

Pressure Gradient

For the pressure gradient, integration by parts over a single element K gives

$$\int_K \mathbf{v} \cdot \nabla p_h d\mathbf{x} = \int_{\partial K} (\mathbf{n}_K \cdot \mathbf{v}) \hat{p}_h \, ds - \int_K (\nabla \cdot \mathbf{v}) p_h \, ds, \quad \mathbf{v} \in \mathbf{V}_h^0 \quad (2.25)$$

The function $\hat{p}_h$ is the numerical trace, which, as in [13], is taken to be

$$\hat{p}_h = \{\!\{p_h\}\!\}, \quad \text{for } e \in \mathcal{E}_h^I; \quad \hat{p}_h = p_h, \quad \text{for } e \in \mathcal{E}_h^B. \quad (2.26)$$

By summing (2.25) over $K \in \mathcal{T}_h$ and employing the key summation formula (2.3), we can get

$$\int_\Omega \mathbf{v} \cdot \nabla_h p_h = \int_{\mathcal{E}_h} \{\!\{\mathbf{v}\}\!\} \cdot [\![\hat{p}_h]\!] + \int_{\mathcal{E}_h^I} [\![\mathbf{v}]\!] \{\!\{\hat{p}_h\}\!\} - \int_\Omega (\nabla_h \cdot \mathbf{v}) p_h \, d\mathbf{x} \quad (2.27)$$

Since $\mathbf{v}$ belongs to $\mathbf{V}_h^0$ which is $H(\mathrm{div})$ conforming with a zero normal component on the boundary and the numerical trace $\hat{p}_h$ is single-valued on edges, we can simplify (2.27) into

$$\int_\Omega \mathbf{v} \cdot \nabla_h p_h = - \int_\Omega p_h \nabla_h \cdot \mathbf{v} \, d\mathbf{x} \quad (2.28)$$

and if we define

$$B_h(\mathbf{v}, q) := -\int_\Omega (\nabla \cdot \mathbf{v}) q \, d\mathbf{x}, \tag{2.29}$$

we have

$$\int_\Omega \mathbf{v} \cdot \nabla p_h \, d\mathbf{x} = B_h(\mathbf{v}, p_h) \tag{2.30}$$

Incompressibility Constraint

By testing the incompressibility constraint (2.1b) against a smooth function $\mathbf{v} \in \mathbf{V}_h^0$ over any element $K \in \mathcal{T}_h$ and by integrating by parts, we have the flux form as below

$$0 = \int_K q \nabla \cdot \mathbf{u}_h \, d\mathbf{x} = -\int_K \mathbf{u}_h \cdot \nabla q \, dx + \int_{\partial K} \hat{\mathbf{u}}_h^p \cdot \mathbf{n}_K q \, ds \tag{2.31}$$

where $\hat{\mathbf{u}}_h^p$ is the numerical trace related with the incompressibility constraint. The following proposition states that if we pick the simplest form for $\hat{\mathbf{u}}_h^p$ and with the inclusion condition (2.21), the approximate velocity is exactly divergence-free with the incompressibility constraint only weakly enforced.

Proposition 2.3.3 *Take the numerical traces $\hat{\mathbf{u}}_h^p$ to be*

$$\hat{\mathbf{u}}_h^p = \{\!\{u_h\}\!\} \quad \text{on } \mathcal{E}_h^I, \quad \hat{\mathbf{u}}_h^p = \mathbf{g} \quad \text{on } \mathcal{E}_h^B \tag{2.32}$$

Then

1. *For $\mathbf{u}_h \in \mathbf{V}_h$ and $\mathbf{q} \in Q_h$, (2.31) can be rewritten into*

$$-B_h(\mathbf{u}_h, q) = 0 \tag{2.33}$$

2. *If $\mathbf{u}_h \in \mathbf{V}_h$ satisfies (2.33) for all $q \in Q_h$, then $\mathbf{u}_h$ is exactly divergence-free, i.e.*

$$\nabla \cdot \mathbf{u}_h \equiv 0, \quad \text{in } \Omega \tag{2.34}$$

Proof: 1) By the summation identity (2.3) we can sum (2.31) over $K \in \mathcal{T}_h$ and get

$$\begin{aligned} 0 &= -\int_\Omega \mathbf{u}_h \cdot \nabla_h q \, dx + \int_{\mathcal{E}_h} \{\!\{\hat{\mathbf{u}}_h^p\}\!\} \cdot [\![q]\!] + \int_{\mathcal{E}_h^I} [[\hat{\mathbf{u}}_h^p]] \, \{\!\{q\}\!\} \\ &= -\int_\Omega \mathbf{u} \cdot \nabla_h q \, dx + \int_{\mathcal{E}_h} \hat{\mathbf{u}}_h^p \cdot [\![q]\!] \, ds \end{aligned} \tag{2.35}$$

Then a second integration by parts of the first term gives

$$\begin{aligned} 0 &= -\left(-\int_\Omega q\nabla\cdot\mathbf{u}_h\,d\mathbf{x}+\int_{\mathcal{E}_h}\{\!\{\mathbf{u}_h\}\!\}\cdot[\![q]\!]+\int_{\mathcal{E}_h^I}[\![\mathbf{u}_h]\!]\,\{\!\{q\}\!\}\right) \\ &\quad +\int_\Gamma \hat{\mathbf{u}}^p\cdot[\![q]\!]\,ds \qquad (2.36) \\ &= \int_\Omega q\nabla\cdot\mathbf{u}_h-\int_{\mathcal{E}^h}\hat{\mathbf{u}}^p\cdot[\![q]\!]-\int_{\mathcal{E}_h^I}0\cdot\{\!\{q\}\!\}+\int_{\mathcal{E}_h}\hat{\mathbf{u}}_h^p\cdot[\![q]\!] \\ &= -B_h(\mathbf{u}_h,q) \qquad (2.37) \end{aligned}$$

2) The inclusion condition (2.21), the divergence theorem, the essential boundary condition in $\mathbf{V}_h$ and the compatibility condition (2.2) give us

$$\nabla\cdot\mathbf{u}_h|_K\in\mathbb{Q}_k(K) \qquad (2.38)$$

$$\int_\Omega\nabla\cdot\mathbf{u}_h\,d\mathbf{x}=\int_\Gamma\mathbf{u}_h\cdot\mathbf{n}\,ds=\int_\Gamma\mathbf{g}\cdot\mathbf{n}\,ds=0. \qquad (2.39)$$

These imply that $\nabla_h\cdot\mathbf{u}_h\in Q_h$, which combined with the fact that

$$-B_h(\mathbf{u}_h,q)=\int_\Omega q\nabla_h\cdot\mathbf{u}_h\,d\mathbf{x}=0,\quad\forall q\in Q_h$$

implies

$$\nabla\cdot\mathbf{u}_h\equiv 0$$

■

The interior penalty DG method for the Stokes problem now consists in finding $(\mathbf{u}_h,p_h)\in\mathbf{V}_h\times Q_h$ which satisfies

$$A_h(\mathbf{u}_h,\mathbf{v})+B_h(\mathbf{v},p_h)=F_h(\mathbf{v}) \qquad (2.40a)$$

$$-B_h(\mathbf{u}_h,q)=0 \qquad (2.40b)$$

for all $(\mathbf{v},q)\in\mathbf{V}_h^0\times Q_h$ and the linear forms are defined as

$$\begin{aligned} A_h(\mathbf{u},\mathbf{v}) &= \int_\Omega\nabla_h\mathbf{u}:\nabla_h\mathbf{v}d\mathbf{x} \\ &+ \frac{\kappa_0}{h}\int_{\mathcal{E}_h^I}\underline{[\![\mathbf{u}]\!]}:\underline{[\![\mathbf{v}]\!]}-\int_{\mathcal{E}_h^I}\underline{[\![\mathbf{u}]\!]}:\{\!\{\nabla_h\mathbf{v}\}\!\}-\int_{\mathcal{E}_h^I}\underline{[\![\mathbf{v}]\!]}:\{\!\{\nabla_h\mathbf{u}\}\!\} \\ &+ \frac{\kappa_0}{h}\int_{\mathcal{E}_h^B}\mathbf{u}\cdot\mathbf{v}-\int_{\mathcal{E}_h^B}(\mathbf{u}\otimes\mathbf{n}):\nabla_h\mathbf{v}-\int_{\mathcal{E}_h^B}(\mathbf{v}\otimes\mathbf{n}):\nabla_h\mathbf{u} \qquad (2.41) \\ B_h(\mathbf{v},q) &= -\int_\Omega q\nabla\cdot\mathbf{v}\,d\mathbf{x} \qquad (2.42) \\ F_h(\mathbf{u}_h) &= \int_\Omega\mathbf{f}\cdot\mathbf{v}d\mathbf{x}-\int_{\mathcal{E}_h^B}(\mathbf{g}\otimes\mathbf{n}):\nabla_h\mathbf{v}\,ds+\frac{\kappa_0}{h}\int_{\mathcal{E}_h^B}\mathbf{g}\cdot\mathbf{v}ds \qquad (2.43) \end{aligned}$$

2.4 Theoretical Analysis

We first introduce the full space

$$\mathbf{U}(h) := H^1(\Omega)^2 + \mathbf{U}_h \tag{2.44}$$

endowed with the DG norm

$$\|\mathbf{v}\|_{1,h}^2 := \sum_{K\in\mathcal{T}_h} \|\nabla \mathbf{v}\|_{0,K}^2 + \sum_{e\in\mathcal{E}_h} \int_e \kappa_0 h^{-1} |\underline{[\![\mathbf{v}]\!]}|^2 \, ds. \tag{2.45}$$

where κ_0 is the penalty parameter independent of h. We also introduce the following subsets of $\mathbf{U}(h)$:

$$\mathbf{V}^0(h) := H^1(\Omega)^2 + \mathbf{V}_h^0 \tag{2.46}$$

$$\mathbf{V}(h) := H^1(\Omega)^2 + \mathbf{V}_h \tag{2.47}$$

To facilitate the analysis of the method we need to introduce an auxiliary space $\underline{\Sigma}_h$ defined by

$$\underline{\Sigma}_K := \{\underline{\tau} \in L^2(\Omega)^{2\times 2} : \underline{\tau} \in \mathbb{Q}_{k+1}(K)^{2\times 2}, \, K \in \mathcal{T}_h\} \tag{2.48}$$

Obviously, we have $\nabla \mathbf{U}_h \subseteq \underline{\Sigma}_h$.

In [3], lifting operators, which lift the edge terms into the cell, are introduced in order to cast all the existing DG methods for elliptic problems into a unified framework. In [37], these operators are further applied to build a unified framework for analysing several DG methods for the saddle-point problems. The idea is to recast the DG methods into a perturbed form with the help of the lifting operators and then derive the abstract error estimates which is a variant of the Strang's lemma. The estimates of jump terms over the edges are converted to those of lifting operators.

Here, we follow [37], for $e \in \mathcal{E}_h$ we introduce the lifting operator $\underline{\mathcal{L}}_e : \mathbf{V}(h) \to \underline{\Sigma}_h$ defined by

$$\int_\Omega \underline{\mathcal{L}}_e(\mathbf{v}) : \underline{\tau} \, d\mathbf{x} = \int_e \underline{[\![\mathbf{v}]\!]} : \{\!\{\underline{\tau}\}\!\} \, ds, \quad \forall \underline{\tau} \in \underline{\Sigma}_h. \tag{2.49}$$

Globally, we define $\underline{\mathcal{L}} : \mathbf{V}(h) \to \underline{\Sigma}_h$ as

$$\underline{\mathcal{L}} := \sum_{e\in\mathcal{E}_h} \underline{\mathcal{L}}_e$$

Then, we define a perturbed form $\tilde{A}_h(\cdot,\cdot)$ basing on the bilinear form $A_h(\cdot,\cdot)$ in (2.41): for $\mathbf{u},\ \mathbf{v} \in \mathbf{V}(h),\ \mathbf{V}^0(h)$

$$\begin{aligned}\tilde{A}_h(\mathbf{u},\mathbf{v}) := &\int_\Omega [\nabla_h \mathbf{u} : \nabla_h \mathbf{v} - \underline{\mathcal{L}}(\mathbf{u}) : \nabla_h \mathbf{v} - \underline{\mathcal{L}}(\mathbf{v}) : \nabla_h \mathbf{u}]\, d\mathbf{x} \\ &+ \kappa \int_{\mathcal{E}_h} \underline{[\![\mathbf{u}]\!]} : \underline{[\![\mathbf{v}]\!]}\, ds. \end{aligned} \tag{2.50}$$

We notice that when restricted to the discrete space $\mathbf{V}_h$, we have

$$\tilde{A}_h(\mathbf{u},\mathbf{v}) = A_h(\mathbf{u},\mathbf{v}), \quad \forall \mathbf{u},\ \mathbf{v} \in \mathbf{V}_h,\ \mathbf{V}_h^0.$$

Hence, using the perturbed form does not change the discrete variational problem (2.40).

2.4.1 Stability Results

Let's first review some useful stability results of the bilinear forms, upon which the proof of the well-posedness and the analysis of the *a priori* error is based. The first result is related to the boundedness and coercivity of the bilinear form $A_h(\cdot,\cdot)$.

Proposition 2.4.1 *For the perturbed form $\tilde{A}_h(\cdot,\cdot)$, there exist constant c_1 and c_2 such that*

$$\begin{aligned} |\tilde{A}_h(\mathbf{u},\mathbf{v})| &\le c_1 \|\mathbf{u}\|_{1,h}\|\mathbf{v}\|_{1,h}, && \forall \mathbf{u} \in \mathbf{V}(h),\ \forall \mathbf{v} \in \mathbf{V}_h^0 \\ \tilde{A}_h(\mathbf{v},\mathbf{v}) &\ge c_2 \|\mathbf{v}\|_{1,h}^2, && \forall \mathbf{u} \in \mathbf{V}_h^0 \end{aligned}$$

Proof: Since $\mathbf{V}_h^0,\ \mathbf{V}_h \subseteq \mathbf{U}_h = \{\mathbf{v} \in L^2(\Omega)^2 : \mathbf{v}|_K \in \mathbb{Q}_{k+1}(K), K \in \mathcal{T}_h\}$, this proposition is a direct consequence of [37, Lemma 7.5, Lemma 7.6]. ■

The next proposition is about the boundedness of $B_h(\mathbf{v},q)$.

Proposition 2.4.2 *The form B_h is continuous*

$$|B_h(\mathbf{v},q)| \le \sqrt{2}\|\mathbf{v}\|_{1,h}\|q\|_0 \quad \forall (\mathbf{v},q) \in \mathbf{V}_0^h \times L^2(\Omega) \tag{2.51}$$

and the velocity-pressure pair $\mathbf{V}_h^0 \times Q_h$ is inf-sup stable

$$\inf_{q \in Q_h} \sup_{\mathbf{v} \in \mathbf{V}_h^0} \frac{B_h(\mathbf{v},q)}{\|\mathbf{v}\|_{1,h}\|q\|_0} \ge \beta > 0 \tag{2.52}$$

for a constant β independent of the mesh size.

Proof: For the continuity, by the definition of $B_h(\cdot,\cdot)$ and ∇_h and the Cauchy-Schwarz inequality, we have

$$\begin{aligned}
|B_h(\mathbf{v},q)| &= \left|\int_\Omega \nabla_h\cdot\mathbf{v}\, q\, d\mathbf{x}\right| = \left|\sum_{K\in\mathcal{T}_h}\int_K \nabla\cdot\mathbf{v}\, q\right| \\
&\le \sum_{K\in\mathcal{T}_h} \|\nabla\cdot\mathbf{v}\|_{0,K}\|q\|_{0,K} \\
&\le \left(\sum_{K\in\mathcal{T}_h}\|\nabla\cdot\mathbf{v}\|_{0,K}^2\right)^{\frac{1}{2}}\left(\sum_{K\in\mathcal{T}_h}\|q\|_{0,K}^2\right)^{\frac{1}{2}} \\
&\le \left(\sum_{K\in\mathcal{T}_h}\int_K 2\sum_{i=1}^{d}(\partial_i v_i)^2\right)^{\frac{1}{2}}\|q\|_0 \\
&\le \sqrt{2}\left(\sum_{K\in\mathcal{T}_h}|\nabla\mathbf{v}|_{1,K}^2\right)^{\frac{1}{2}}\|q\|_0 \\
&\le \sqrt{2}\|\mathbf{v}\|_{1,h}\|q\|_0
\end{aligned}$$

The proof of the inf-sup condition can be found in [37, Theorem 6.12]. ■

It is easy to verify that the stability results in this section imply the unique solvability of the approximation problem (2.40).

2.4.2 Error Estimates

The *a priori* error estimate is based on an abstract error estimate and some standard approximation results. We make the regularity assumption that the exact solution $(\mathbf{u},p)$ of the Stokes system (2.1) satisfies

$$(\mathbf{u},p)\in H^{s+1}(\mathcal{T}_h)^2\times H^s(\mathcal{T}_h),\quad s\ge 1 \tag{2.53}$$

and $\mathbf{u}|_\Gamma=\mathbf{g}$ where $H^r(\mathcal{T}_h)$, for $r>0$, is the broken Sobolev space with the definition

$$H^r(\mathcal{T}_h)=\{v\in L^2(\Omega):\ v|_K\in H^r(K),\ K\in\mathcal{T}_h\} \tag{2.54}$$

Abstract Error Estimate

We follow [37] and [13] and first present the abstract error estimate in terms of the expression

$$\mathcal{R}_h(\mathbf{u},p;\mathbf{v}):=\sup_{\mathbf{0}\neq\mathbf{v}\in\mathbf{V}_h^0}\frac{|R_h(\mathbf{u},p;\mathbf{v})|}{\|\mathbf{v}\|_{1,h}} \tag{2.55}$$

where the residual $R_h(\mathbf{u}, p; \mathbf{v})$ is defined as

$$R_h(\mathbf{u}, p; \mathbf{v}) = \tilde{A}_h(\mathbf{u}, \mathbf{v}) + B_h(\mathbf{v}, p) - F_h(\mathbf{v}) \tag{2.56}$$

for $\mathbf{v} \in \mathbf{V}_h^0$.

We need to emphasize that, due to the introduction of the perturbed form $\tilde{A}_h$, we can not conclude that $R_h(\mathbf{u}, p; \mathbf{v}) = 0$ in general. The reason for this is that the term $\underline{\mathcal{L}}(\mathbf{v}) : \nabla_h \mathbf{u}$ is inconsistent since $\nabla_h \mathbf{u} \notin \underline{\Sigma}_h$. In the next proposition, we will see that the residual is actually optimally convergent.

Proposition 2.4.3 *Assume that the exact solution $(\mathbf{u}, p)$ of the Stokes system (2.1) satisfy (2.53). Let $\underline{Q}$ and Q be the L^2 projections onto $\underline{\Sigma}_h$ and Q_h, respectively. Then the residual in $R_h(\mathbf{u}, p; \mathbf{v})$ is given by*

$$R_h(\mathbf{u}, p; \mathbf{v}) = \int_{\mathcal{E}_h} \{\!\{\nabla \mathbf{u} - \underline{Q}(\nabla \mathbf{u})\}\!\} : \underline{[\![\mathbf{v}]\!]}\, ds, \quad \forall \mathbf{v} \in \mathbf{V}_h^0 \tag{2.57}$$

Moreover, we have that

$$\mathcal{R}_h(\mathbf{u}, p)^2 \leq C h^{2\min(s,k)} \|\mathbf{u}\|_{s+1}^2 \tag{2.58}$$

with a constant $C > 0$ independent of h.

Proof: The proof can be found in [37, Proposition 8.1]. ■

In the next proposition we present the abstract error estimate which is a variant of Strang's lemma.

Proposition 2.4.4 *Let $(\mathbf{u}, p) \in \mathbf{V} \times Q$ be the exact solution of the Stokes problem and $(\mathbf{u}_h, p_h) \in \mathbf{V}_h \times Q_h$ the approximate solution of the DG problem (2.40). We have*

$$\|\mathbf{u} - \mathbf{u}_h\|_{1,h} \leq C_u \left[\inf_{\mathbf{v} \in \mathbf{V}_h} \|\mathbf{u} - \mathbf{v}\|_{1,h} + \inf_{q \in Q_h} \|p - q\|_0 + \mathcal{R}_h(\mathbf{u}, p) \right] \tag{2.59}$$

$$\|p - p_h\|_0 \leq C_p \left[\inf_{q \in Q_h} \|p - q\|_0 + \|\mathbf{u} - \mathbf{u}_h\|_{1,h} + \mathcal{R}_h(\mathbf{u}, p) \right] \tag{2.60}$$

where C_u, $C_p > 0$ only depend on the stability parameters.

Proof: The proof can be found in [37, Proposition 4.1] and is based on the stability results of the bilinear forms $A_h(\cdot, \cdot)$ and $B_h(\cdot, \cdot)$. ■

To prove the *a priori* estimate we need the following standard results:

Lemma 2.4.5 *[8, Proposition 3.6] Let K be an affine element and $W(K) = \{\mathbf{v} \in \mathbf{L}^r(K))|\nabla\cdot\mathbf{v} \in L^2(\Omega)\}$, $r > 2$. The interpolant operator mapping $\rho_K : W(K) \to \mathbf{RT}_k(K)$ is defined to be $\rho_K\mathbf{v} = \widehat{\mathbf{\Pi}}_k\hat{\mathbf{v}} \circ \mathcal{P}_K^{-1}$ where $\hat{\mathbf{v}} = \mathbf{v} \circ \mathcal{P}_K$. There exists a constant c depending only on k and on the shape of K, such that, for any $\mathbf{v} \in \mathbf{H}^{s+1}(K)$, we have*

$$\|\mathbf{v} - \rho_K\mathbf{v}\|_{0,K} \leq ch_K^{\min\{s,k\}+1}|\mathbf{v}|_{s+1,K} \tag{2.61}$$

$$\|\mathbf{v} - \rho_K\mathbf{v}\|_{1,K} \leq ch_K^{\min\{s,k\}}|\mathbf{v}|_{s+1,K} \tag{2.62}$$

■

The last lemma will help us deal with jump terms in the definition of the $\|\cdot\|_{1,h}$, as we will see in the proof of Theorem 2.4.7.

Lemma 2.4.6 *[36, Lemma 1.2.14] For any function $u \in H^1(\mathcal{T}_h)$, we have*

$$\|u\|_{0,\partial K} \leq C(h_K^{1/2}|u|_{1,K} + h_K^{-1/2}\|u\|_{0,K}) \tag{2.63}$$

where K is any element in $\mathcal{T}_h$ and constant $C > 0$ independent of meshsize.

Then based on this we are ready to state the *apriori* error estimate result

Theorem 2.4.7 (a priori error estimate) *Let $(\mathbf{u}, p)$ be the exact solution of the Stokes problem satisfying the regularity assumption (2.53) and $(\mathbf{u}_h, p_h) \in \mathbf{V}_h \times Q_h$ the finite element approximation. We have the following error estimates*

$$\|\mathbf{u} - \mathbf{u}_h\|_h \leq Ch^{\min\{s,k\}}\|\mathbf{u}\|_{s+1} \tag{2.64}$$

$$\|p - p_h\|_0 \leq Ch^{\min\{s,k\}}\|\mathbf{u}\|_{s+1} \tag{2.65}$$

where the constant $C > 0$ independent of h. ■

Proof: By the standard approximation estimates for the L^2-projection (see [20, Appendix A]) and Proposition 2.4.3 we have

$$\inf_{q\in\mathcal{Q}_h} \|p - q\|_0 \leq Ch^{\min\{s,k+1\}}\|q\|_s \tag{2.66}$$

$$\mathcal{R}_h(\mathbf{u}, p) \leq Ch^{\min\{s,k\}}\|\mathbf{u}\|_{s+1} \tag{2.67}$$

According to the abstract error estimates (2.59) and (2.60), it then remains to bound the infimum $\inf_{\mathbf{v}\in\mathbf{V}_h} \|\mathbf{u}-\mathbf{v}\|_{1,h}$. We take $\mathbf{v} = \mathbf{\Pi}\mathbf{u}$, where $\mathbf{\Pi}$ is the global interpolation operator mapping from $H(\mathrm{div}, \Omega) \cap (\mathrm{L}^{\mathrm{r}}(\Omega))^{\mathrm{d}}$ r > 2, into $\mathbf{RT}_k(\Omega, \mathcal{T}_h) := \{\mathbf{v} \in H(\mathrm{div}, \Omega),\ \mathbf{v}|_{\mathrm{K}} \in \mathbf{RT}_{\mathrm{k}}(\mathrm{K})\}$ by setting

$$\Pi\mathbf{u}|_K = \rho_K\mathbf{u}$$

where ρ_K is the local interpolant operator defined in Lemma 2.4.5. By (2.12), the definition of the Raviart-Thomas interpolation operator $\widehat{\mathbf{\Pi}}$ in (2.13) and the property of the Piola transformation (2.17), it is not hard to see that $\mathbf{\Pi u} \in \mathbf{V}_h$.

If we set $\xi_{\mathbf{u}} = \mathbf{u} - \Pi\mathbf{u}$, then by Lemma 2.4.5, Cauchy-Schwarz inequality and by applying Lemma 2.4.6 to each component we can get

$$\begin{aligned}
\|\xi_{\mathbf{u}}\|_{1,h}^2 &= \sum_{K\in\mathcal{T}_h} |\xi_{\mathbf{u}}|_{1,K}^2 + \int_{\mathcal{E}} \kappa |\, [\![\xi_{\mathbf{u}} \otimes \mathbf{n}]\!] \,|^2 \, ds \\
&\leq \sum_{K\in\mathcal{T}_h} \|\xi_{\mathbf{u}}\|_{1,K}^2 + \sum_{K\in\mathcal{T}_h} \int_{\partial K} \kappa_0 h_K^{-1} |\xi_{\mathbf{u}} \otimes \mathbf{n}|^2 \, ds \\
&\leq Ch^{2\min\{s,k\}} \|\mathbf{u}\|_{s+1}^2 + \sum_{K\in\mathcal{T}_h} \kappa_0 h_K^{-1} \|\xi_{\mathbf{u}}\|_{0,\partial K}^2 \\
&\leq Ch^{2\min\{s,k\}} \|\mathbf{u}\|_{s+1}^2 + \sum_{K\in\mathcal{T}_h} C(h_K |\xi_{\mathbf{u}}|_{1,K}^2 + h_K^{-1} \|\xi_{\mathbf{u}}\|_{0,K}^2) \\
&\leq Ch^{2\min\{s,k\}} \|\mathbf{u}\|_{s+1}^2 + \sum_{K\in\mathcal{T}_h} Ch_K^{2\min\{s,k\}+1} \|\mathbf{u}\|_{s+1,K}^2 \\
&\leq Ch^{2\min\{s,k\}} \|\mathbf{u}\|_{s+1}^2
\end{aligned}$$

which implies

$$\inf_{\mathbf{v}\in\mathbf{V}_h} \|\mathbf{u} - \mathbf{v}\|_h \leq \|\mathbf{e}_\xi\|_h \leq Ch^s \|\mathbf{u}\|_{s+1} \tag{2.68}$$

Then by combining the abstract error estimates and the approximation results (2.67), (2.66) we can get the *a priori* error estimates (2.64),(2.65). ■

2.5 Numerical Experiment

In this section numerical experiments are conducted with the *deal.II* finite element library [5]. We test the method with the Kovasznay Flow [28]; see also the numerical experiments in [13] and [14]. The computational domain is taken to be

$$\Omega = \left[-\frac{1}{2}, \frac{3}{2}\right] \times [0, 2]$$

and is covered by a uniform rectangular mesh. At level l, the meshsize is $h = 2^{-l}$. We prescribe the analytical solution

$$\begin{aligned}
u_1(x, y) &= 1 - e^{\lambda x} \cos(2\pi y), \\
u_2(x, y) &= \frac{\lambda}{2\pi} e^{\lambda x} \sin(2\pi y). \\
p(x, y) &= -\frac{1}{2} e^{2\lambda x} - \bar{p}
\end{aligned}$$

where

$$\lambda = \frac{-8\pi^2}{\nu^{-1} + \sqrt{\nu^{-2} + 16\pi^2}}$$

The viscosity ν is taken to be 1 and the corresponding right hand side is

$$\mathbf{f} = \begin{pmatrix} (\lambda^2 - 4\pi^2)e^{\lambda x}\cos(2\pi y) - \lambda e^{2\lambda x} \\ \\ (2\pi\lambda - \frac{\lambda^3}{2\pi})e^{\lambda x}\sin(2\pi y) \end{pmatrix}$$

In this experiment the penalty parameter is chosen to be

$$\kappa_0 = 2k(k+3)$$

As emphasized in [14], the normal component of the inhomogeneous Dirichlet boundary condition is interpolated in a strong way on a set of quadrature points on which the $\mathbf{RT}_k$ moments are integrated exactly. The L_2-norm error for the pressure and the velocity as

k	cycle	$\|e_p\|_0$		$\|e_{\mathbf{u}}\|_0$		$\|e_{\mathbf{u}}\|_{1,h}$		$\|\nabla \cdot \mathbf{u}_h\|_\infty$
k=1	4	4.543e-01	1.08	8.733e-03	1.99	1.631e+00	1.64	1.705e-13
	5	1.928e-01	1.24	2.227e-03	1.97	6.964e-01	1.23	5.116e-13
	6	7.071e-02	1.45	5.660e-04	1.98	3.254e-01	1.10	1.020e-12
	7	2.339e-02	1.60	1.431e-04	1.98	1.571e-01	1.05	3.197e-12
k=2	1	1.945e+00	-	6.433e-02	-	6.954e+00	-	5.826e-13
	2	3.307e-01	2.56	7.889e-03	3.03	1.225e+00	2.50	1.070e-12
	3	4.675e-02	2.82	9.562e-04	3.04	3.099e-01	1.98	2.727e-12
	4	6.343e-03	2.88	1.166e-04	3.04	7.919e-02	1.97	5.177e-12
	5	8.816e-04	2.85	1.436e-05	3.02	2.005e-02	1.98	1.013e-11
	6	1.290e-04	2.77	1.780e-06	3.01	5.047e-03	1.99	3.980e-11
k=3	1	3.627e-01	-	5.738e-03	-	4.281e-01	-	1.495e-12
	2	3.243e-02	3.48	3.689e-04	3.96	4.260e-02	3.33	4.182e-12
	3	2.424e-03	3.74	2.318e-05	3.99	4.698e-03	3.18	7.731e-12
	4	1.799e-04	3.75	1.450e-06	4.00	5.471e-04	3.10	2.009e-11
	5	1.421e-05	3.66	9.070e-08	4.00	6.481e-05	3.08	5.423e-11
k=4	1	5.201e-02	-	3.950e-04	-	3.961e-02	-	2.087e-12
	2	2.312e-03	4.49	1.219e-05	5.02	2.846e-03	3.80	5.684e-12
	3	8.393e-05	4.78	3.782e-07	5.01	1.824e-04	3.96	1.695e-11
	4	2.943e-06	4.83	1.177e-08	5.01	1.143e-05	4.00	2.846e-11
	5	1.068e-07	4.78	3.670e-10	5.00	7.144e-07	4.00	6.732e-11

Table 2.1: Numerical results for Kovasznay flow ($\nu = 1$)

well as the error in DG-norm for the velocity are listed in Table 2.5.1 for polynomials of

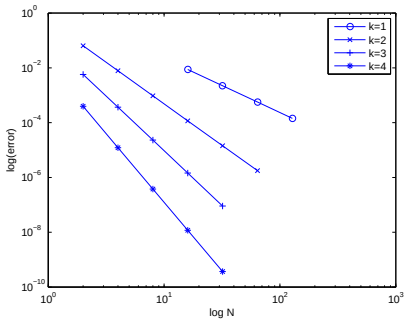

(a) convergent plot for $\|\mathbf{e_u}\|_0$

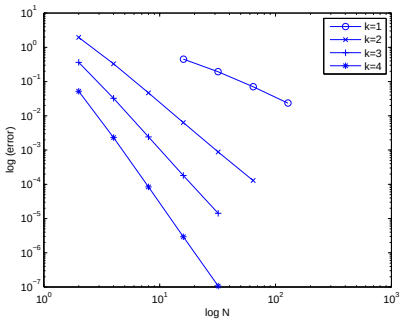

(b) convergent plot for$\|e_p\|_0$

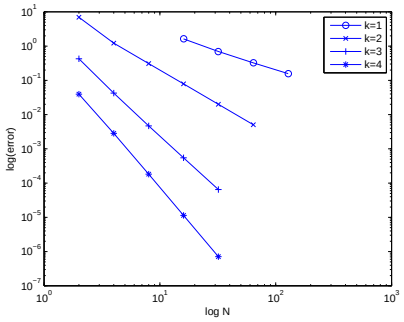

(c) convergent plot for$\|\mathbf{e_u}\|_{1,h}$

Figure 2.2: The convergent plots for the numerical errors

degree $k = 1, ..., 4$. The convergence plots are presented in Figure 2.2. We observe optimal orders of convergence for the error of the velocity in both norms, while for the pressure the orders of convergence in the L^2-norm are much better than expected in Theorem 2.4.7. This is also observed in [14]. The reason for this is that the abstract error estimate for the pressure (2.60) is bounded by the error of the velocity in $\|\cdot\|_{1,h}$ norm, which is of order $O(h^k)$. However, in L^2-norm, the optimal approximation order of the space $\mathbb{Q}_k$ should be $O(h^{k+1})$. Therefore, an order between $O(h^k)$ and $O(h^{k+1})$ is observed. Moreover, the divergence of the approximate velocity in the L^∞-norm is evaluated at a set of $(k+1)^2$ quadrature points in each element K. We see from the last column in the Table 2.5.1 that the approximate velocity is exactly divergence-free.

Chapter 3

Non-isothermal Problem

3.1 Introduction

When a fluid is subjected to a temperature change, its material properties, such as density and viscosity, changes accordingly. If these changes are large enough to have a substantial influence on the flow field, the flow is considered to be *non-isothermal*. The numerical simulation of the non-isothermal incompressible flow has received much attention recently in both natural sciences and engineering branches. Relevant industrial applications include polymer processing, cooling processes, the design of heat exchangers and chemical reactors; see e.g. [30], [26] and [35]. Moreover, in geophysics, the convection processes in the Earth's mantle are well described by incompressible fluid flow driven by temperature-induced small density differences; see [29]. The numerical simulation of these processes is a key piece in understanding the dynamics, composition, history and interaction between the mantle and the lithosphere.

In the last decade many finite element methods have been developed and analysed for such problems. In [15], a mixed finite element method is developed for the non-isothermal Stokes-Oldroyd equations. For the same problem, a dual mixed finite element is constructed and analysed in [19], which has properties analogous to finite volume methods, namely, local conservation of momentum and mass. In [18] a conforming finite element method is presented and analysed for approximating time-dependent non-isothermal incompressible flow problems. The time is disretized by the backward Euler method. But none of these methods have the exactly divergence-free property as our approach does.

In this chapter, we first illustrate how the non-isothermal effects are introduced into the equations by reviewing two classical physical models. Then we review the work of [34] which extends the exactly divergence-free element developed in [13] and [14] to a generalized Boussinesq system. The model problem couples the stationary incompressible

Navier-Stokes equation and a convection-diffusion equation. The coupling is through a temperature-dependent viscosity, which is also nonlinear, and through a buoyancy term acting in the opposite direction of gravity.

We extend the IPDG method described in Chapter 1 to this coupled system and by doing so, the exactly divergence-free constraint is preserved on the discrete level. The formulation of the numerical method and the *a priori* error estimate are first reviewed. Then numerical examples are implemented to verify the theoretical results.

3.2 Physical Models

In this section, we briefly discuss the physical approximations that introduce the non-isothermal effects into incompressible flow models. The first one is the constitute relation of the Oldroyd-B type for modelling the viscoelastic problems. The second one is the Boussinesq approximation for linearizing buoyancy effect when considering the buoyancy driven flows. These two modelling techniques are introduced separately in the context of two different models.

3.2.1 Model I: Non-Isothermal Stokes-Oldroyd System

The viscoelastic problem occurs in a variety of applications, including polymer processing. The complexity of the governing equations makes both the mathematical analysis and the associated numerical methods especially difficult. The current effort is to model viscoelastic flows as the solution of a modified Stokes problem; see [6, 10]. In [15], the non-isothermal Stokes problem is modified in the same way as in [6].

We consider a fluid flowing in a bounded and connected domain $\Omega \in \mathbb{R}^2$, whose boundary is denoted by Γ and we assume the stationary and creeping flow hypothesis. Let the velocity be denoted by $\mathbf{u}$, pressure by p, extra stress tensor by $\underline{\sigma}$, rate of strain tensor by $\underline{D}(\mathbf{u}) = \frac{1}{2}(\nabla\mathbf{u} + \nabla\mathbf{u}^T)$ and temperature by T. In the Oldroyd-B model the extra stress tensor is split into the Newtonian solvent part $\underline{\sigma}_s = \alpha_s \underline{D}(\mathbf{u})$ and the non-Newtonian polymer part $\underline{\sigma}_p$, i.e.

$$\underline{\sigma} = \underline{\sigma}_s + \underline{\sigma}_p.$$

$\underline{\sigma}_p$ is given by

$$\underline{\sigma}_p + We\frac{\partial_a \underline{\sigma}_p}{\partial t} = 2\alpha\underline{D}(\mathbf{u}); \quad a \in [-1,1], \alpha \in (0,1) \tag{3.1}$$

where W_e is the Weissenberg number and the derivative $\frac{\partial_a \underline{\sigma}_p}{\partial t}$ is defined by

$$\frac{\partial \underline{\tau}}{\partial t} = \underline{\tau}_t + (\mathbf{u}\cdot\nabla)\underline{\tau} + g_a(\underline{\tau}, \nabla\mathbf{u}), \quad a \in [-1,1] \tag{3.2}$$

and

$$g_a(\underline{\tau}, \nabla \mathbf{u}) = \underline{\sigma\omega}(\mathbf{u}) - \underline{\omega}(\mathbf{u})\underline{\sigma} - a(\underline{D}(u)\underline{\sigma} + \underline{\sigma}\,\underline{D}(u)).$$

This is a variation of the upper-convected time derivative (see [27]), which is the material derivative of the tensor property in the coordinate system rotating and stretching with the fluid.

In the limit case $W_e = 0$ we can get the Oldroyd-Stokes problem

$$\begin{aligned} -\nabla \cdot [(2\alpha_p + 2\epsilon\alpha_s)\underline{D}(\mathbf{u})] + \nabla p &= \mathbf{f}_1 \quad \text{in } \Omega \\ \nabla \cdot \mathbf{u} &= 0 \quad \text{in } \Omega \\ \mathbf{u} &= \mathbf{g}_1 \quad \text{on } \Gamma \end{aligned} \tag{3.3}$$

where α_p and α_s are the polymetric viscosity and the solvent one respectively and $\epsilon > 0$ is a small parameter that makes the effect of α_s much smaller than that of α_p.

Many flows of interest in polymetric melt processing are non-isothermal. We follow the derivation in [15] for the non-isothermal Oldroyd-Stokes system. By introducing temperature-dependent coefficients $\alpha_p(T)$ and $\alpha_s(T)$ and by combining the Oldroyd-Stokes system (3.3) and a convection-diffusion equation for the temperature, we can obtain

$$\begin{aligned} -\nabla \cdot [(2\alpha_p(T) + 2\epsilon\alpha_s(T)\underline{D}(\mathbf{u})] + \nabla p &= \mathbf{f}_1 \quad \text{in } \Omega \\ \nabla \cdot \mathbf{u} &= 0 \quad \text{in } \Omega \\ -\eta\Delta T + \mathbf{u} \cdot \nabla T &= f_2 \quad \text{in } \Omega \\ \mathbf{u} &= \mathbf{g}_1 \quad \text{on } \Gamma \\ T &= g_2 \quad \text{on } \Gamma \end{aligned} \tag{3.4}$$

where η is the thermal conductivity coefficient, $\mathbf{f}_1$ is the body force, f_2 the heat source. The dependence of the polymer and solvent viscosity on the temperature is given by the Arrhenius equations (see [25]):

$$\alpha_p(T) = a_1 \exp\left(\frac{b_1}{T}\right), \;\; \alpha_s(T) = a_2 \exp\left(\frac{b_2}{T}\right), \; b_1 \neq 0. \tag{3.5}$$

The constants a_i, b_i, $i = 1, 2$ are chosen such that

$$0 < \alpha_s \leq 1, \quad 0 < \alpha_s < 1$$

3.2.2 Model II: Buoyancy Driven Flows

If the fluid density varies with temperature, a flow can be induced in the presence of gravity. This is known as buoyancy-driven flow. Many flow phenomena are driven by buoyancy, and such flows are especially important in the modelling of the convection processes in the Earth's mantle; see [38] . When the viscous friction forces in the fluids are large compared to buoyancy forces, for example when simulating the mantle, the motion of the fluid is slow and inertial terms can be neglected; see [29] and the book [38]. Combining this with the steady-state assumption, we obtain governing equations in the following form

$$\begin{aligned} -\nabla \cdot (2\alpha \underline{D}(\mathbf{u})) + \nabla p &= \mathbf{g}\,\rho(T) && \text{in } \Omega \\ \nabla \cdot \mathbf{u} &= 0 && \text{in } \Omega \\ -\nabla \cdot \eta \nabla T + \mathbf{u} \cdot \nabla T &= f_2 && \text{in } \Omega \\ \mathbf{u} &= \mathbf{g}_1 && \text{on } \Gamma \\ T &= g_2 && \text{on } \Gamma \end{aligned} \tag{3.6}$$

where α is the viscosity, $\mathbf{g}$ the gravity acceleration, $\rho(T)$ the temperature-dependent density. Other notations are the same as those in last section.

The standard assumption made to simplify the analysis of the system above is the Boussinesq approximation, in which the density differences are neglected, except in the buoyancy term, where they appear in terms multiplied by $\mathbf{g}$. If all accelerations involved in the flow are small compared to $\mathbf{g}$, the dependence of the density on T in the buoyancy term can be assumed to be linear:

$$\rho(T) - \rho_0 = -\rho_0 \beta (T - T_0).$$

Here, T_0 is a reference temperature, e.g., the temperature on a boundary, and β is the coefficient of expansion for the fluid. The corresponding buoyancy force is then given as

$$\mathbf{f}_B = -\rho_0 \mathbf{g} \beta (T - T_0).$$

Then the nonlinear equation of the conservation of momentum can be linearized into

$$-\nabla \cdot (2\alpha \underline{D}(\mathbf{u})) + \nabla p = \mathbf{g}\rho_0(1 - \beta(T - T_0)) - \rho_0 \mathbf{g} \beta T$$

If we express the gravity in the potential form $\mathbf{g} = -\nabla\phi$ and introduce the effective pressure $p_{eff} = p + \phi\rho_0(1 - \beta(T - T_0))$, the equation above can be further rewritten as

$$-\nabla \cdot (2\alpha \underline{D}(\mathbf{u})) + \nabla p_{\text{eff}} = -\rho_0 \mathbf{g} \beta T.$$

3.3 Model Problem

In this section, to ease the mathematical analysis, we consider the following generalized model problem, which captures all the non-isothermal effects, with zero heat source and homogeneous velocity field on the boundary:

$$-\nabla \cdot (\alpha(T)\nabla \mathbf{u}) + \mathbf{u} \cdot \nabla \mathbf{u} + \nabla p = \mathbf{j}\, T \qquad \text{in } \Omega \tag{3.7a}$$

$$\nabla \cdot \mathbf{u} = 0 \qquad \text{in } \Omega \tag{3.7b}$$

$$-\nabla \cdot (\eta(T)\nabla T) + \mathbf{u} \cdot \nabla T = 0 \qquad \text{in } \Omega \tag{3.7c}$$

$$\mathbf{u} = \mathbf{0} \qquad \text{on } \Gamma \tag{3.7d}$$

$$T = g_T \qquad \text{on } \Gamma \tag{3.7e}$$

where Ω is the computational domain in $\mathbb{R}^2$ and T is the temperature, $\mathbf{u}$ the velocity, p the pressure, $\mathbf{j} \in \mathbf{L}^2(\Omega)$ is a constant vector in the opposite direction of the gravity acceleration. The boundary datum g_T is assumed to be in $C(\bar{\Gamma})$. For the rest of this chapter, we will use the same notations for the mesh, function spaces and numerical traces as those defined in Chapter 1.

The temperature-dependent parameters $\alpha(T)$ and $\eta(T)$ denote the effective viscosity and heat conductivity, respectively. We assume they are Lipschitz continuous and bounded, that is

$$|\alpha(T_1) - \alpha(T_2)| \leq L_\alpha |T_1 - T_2|, \quad |\eta(T_1) - \eta(T_2)| \leq L_\eta |T_1 - T_2| \tag{3.8}$$

for all values of T_1 and T_2, with the Lipschitz constants L_α, $L_\eta > 0$. And there exist constants α_1, α_2, η_1, $\eta_2 > 0$, such that

$$0 < \alpha_1 \leq \alpha(T) \leq \alpha_2, \quad 0 < \eta_1 \leq \eta(T) \leq \eta_2 \tag{3.9}$$

for all T.

The variational formulation of the problem (3.7) is to find $(\mathbf{u}, p, T) \in H^1(\Omega)^2 \times L^2_0(\Omega) \times H^1(\Omega)$ with $T|_\Gamma = g_T$, such that

$$A(\mathbf{u}, \mathbf{v}; T) + B(\mathbf{v}, p) + O_N(\mathbf{u}, \mathbf{v}; \mathbf{u}) - D(T, \mathbf{v}) = \mathbf{0} \tag{3.10a}$$

$$-B(\mathbf{u}, q) = 0 \tag{3.10b}$$

$$C(T, S; T) + O_H(T, S; \mathbf{u}) = 0 \tag{3.10c}$$

for all $(\mathbf{v}, q, S) \in H_0^1(\Omega)^2 \times L_0^2(\Omega) \times H_0^1(\Omega)$, and where the bilinear and linear forms are

$$A(\mathbf{u}, \mathbf{v}; O) = \int_\Omega \alpha(O) \nabla \mathbf{u} : \mathbf{v} d\,\mathbf{x} \qquad B(\mathbf{v}, q) = \int_\Omega (\nabla_h \cdot \mathbf{u}) q \, d\mathbf{x}$$
$$O_N(\mathbf{u}, \mathbf{v}; \mathbf{w}) = \int_\Omega (\mathbf{w} \cdot \nabla)\mathbf{u} \cdot \mathbf{v} \, d\mathbf{x} \qquad O_H(T, S; \mathbf{u}) = \int_\Omega (\mathbf{u} \cdot \nabla T) S \, dx$$
$$D(T, \mathbf{v}) = \int_\Omega T\mathbf{j} \cdot \mathbf{v} \, d\mathbf{x} \qquad C(T, S; O) = \int_\Omega \eta(O) \nabla T \cdot \nabla S \, dx$$

3.3.1 Stability Results

First, let us review some stability results of the forms appearing in (3.10) from [34].

Boundedness and Continuity

Due to the assumption (3.9), we have the following continuity properties:

$$|A(\mathbf{u}, \mathbf{v}; \cdot) \le \alpha_2 \|\mathbf{u}\|_{1,\Omega} \|\mathbf{v}\|_{1,\Omega}, \qquad \mathbf{u}, \mathbf{v} \in H^1(\Omega)^2, \tag{3.11}$$
$$|C(T, S; \cdot)| \le \eta_2 \|T\|_{1,\Omega} \|S\|_{1,\Omega}, \qquad T, S \in H^1(\Omega), \tag{3.12}$$
$$|B(\mathbf{v}, q)| \le C_B \|\mathbf{v}\|_{1,\Omega} \|q\|_{0,\Omega}, \qquad \mathbf{v} \in H^1(\Omega)^2,\ q \in L^2(\Omega). \tag{3.13}$$

Moreover, from the Lipschitz continuity of α and η in (3.8) and Hölder's inequality, the following Lipschitz continuity properties hold for the form A and C: for T_1, $T_2 \in H^1(\Omega)$, $\mathbf{u} \in W^{1,\infty}(\Omega)$, $T \in W^{1,\infty}(\Omega)$, we have

$$|A(\mathbf{u}, \mathbf{v}; T_1) - A(\mathbf{u}, \mathbf{v}; T_2)| \le L_A \|\mathbf{u}\|_{\mathbf{W}^{1,\infty}(\Omega)} \|T_1 - T_2\|_{1,\Omega} \|\mathbf{v}\|_{1,\Omega}, \quad \mathbf{v} \in \mathbf{H}^1(\Omega) \tag{3.14}$$
$$|C(T, S; T_1) - C(T, S; T_2)| \le L_T \|T\|_{W^{1,\infty}(\Omega)} \|T_1 - T_2\|_{1,\Omega} \|S\|_{1,\Omega}, \quad S \in H^1(\Omega) \tag{3.15}$$

Due to Hölder's inequality and the standard Sobolev embeddings, the trilinear forms O_N and O_H have the following bounds:

$$|O_N(\mathbf{u}, \mathbf{v}; \mathbf{w})| \le C_N \|\mathbf{w}\|_{1,\Omega} \|\mathbf{u}\|_{1,\Omega} \|\mathbf{v}\|_{1,\Omega}, \qquad \mathbf{w}, \mathbf{u}, \mathbf{v} \in \mathbf{H}^1(\Omega) \tag{3.16}$$
$$|O_H(T, S; \mathbf{w})| \le C_H \|\mathbf{w}\|_{1,\Omega} \|T\|_{1,\Omega} \|S\|_{1,\Omega}, \qquad \mathbf{w} \in \mathbf{H}^1(\Omega),\ T, S \in H^1(\Omega) \tag{3.17}$$

Also, we have the bound on D

$$|D(T, \mathbf{v})| \le C_D \|\mathbf{j}\|_{0,\Omega} \|T\|_{1,\Omega} \|\mathbf{v}\|_{1,\Omega}, \quad \theta \in H^1(\Omega),\ \mathbf{v} \in \mathbf{H}^1(\Omega) \tag{3.18}$$

Coercivity and Inf-sup condition

Next, we review the coercivity of the linear forms. By the Poincaré inequality and the bounds in (3.9), we have

$$A(\mathbf{u}, \mathbf{u}; \cdot) \ge \alpha_A \|\mathbf{u}\|_{1,\Omega}^2, \qquad \mathbf{v} \in \mathbf{H}_0^1(\Omega), \tag{3.19}$$
$$C(T, T; \cdot) \ge \alpha_C \|T\|_{1,\Omega}, \qquad T \in H_0^1(\Omega) \tag{3.20}$$

To discuss the coercivity of the forms O_H and O_N, we need to introduce the kernel

$$\mathbf{X} = \{\mathbf{v} \in \mathbf{H}^1(\Omega) : \ B(\mathbf{v}, q) = 0, \ \forall q \in L_0^2(\Omega)\} = \{\mathbf{v} \in \mathbf{H}^1(\Omega) : \ \nabla \cdot \mathbf{v} \equiv 0\} \tag{3.21}$$

Then integration by parts gives us,

$$O_N(\mathbf{u}, \mathbf{u}; \mathbf{w}) = 0, \qquad \mathbf{w} \in \mathbf{X}, \ \mathbf{v} \in \mathbf{H}^1(\Omega) \tag{3.22}$$

$$O_H(T, T; \mathbf{w}) = 0, \qquad \mathbf{w} \in \mathbf{X}, \ T \in H^1(\Omega) \tag{3.23}$$

Finally the bilinear form B satisfies the continuous inf-sup condition

$$\sup_{\mathbf{v} \in \mathbf{H}_0^1(\Omega) \setminus \{\mathbf{0}\}} \frac{B(\mathbf{v}, q)}{\|\mathbf{v}\|_{1,\Omega}} \geq \beta \|q\|_{0,\Omega}, \qquad \forall q \in L_0^2(\Omega) \tag{3.24}$$

with an inf-sup constant $\beta > 0$ only depending on Ω; see [20].

3.3.2 Unique Solvability

In this section, we review the results related to the existence and uniqueness of the solution to the system (3.7). To that end, it's enough to study the reduced problem on the kernel $\mathbf{X}$ which is defined in (3.21). The reduced problem consists of finding $(\mathbf{u}, p) \in \mathbf{V} \times H^1(\Omega)$ such that $T|_\Gamma = g_T$ and

$$A(\mathbf{u}, \mathbf{v}; T) + O_N(\mathbf{u}, \mathbf{v}; \mathbf{u}) - D(T, \mathbf{v}) = 0, \tag{3.25a}$$

$$C(T, S; T) + O_H(T, S; \mathbf{u}) = 0 \tag{3.25b}$$

for all $(\mathbf{v}, T) \in \mathbf{X} \times H_0^1(\Omega)$.

First, we have the following equivalence property; see [20], which justifies our consideration of the reduced problem.

Lemma 3.3.1 *If $(\mathbf{u}, p, T) \in \mathbf{H}^1(\Omega) \times L_0^2\Omega \times H^1(\Omega)$ is a solution of (3.10), then $\mathbf{u} \in \mathbf{X}$ and $(\mathbf{u}, T)$ is also a solution of (3.25). Conversely, if $(\mathbf{u}, T) \in \mathbf{X} \times H^1(\Omega)$ is a solution of (3.25), then there exists a unique pressure $p \in L_0^2(\Omega)$ such that $(\mathbf{u}, p, T)$ is a solution of (3.28).*

The next theorem ensures the solvability of the reduced problem (3.25).

Theorem 3.3.2 (Solvability) *Assume (3.9) and (3.8). Then for any $\mathbf{j} \in \mathbf{L}^2(\Omega)$, there exists a lifting $T_1 \in H^1(\Omega)$ of $g_1 \in H^{1/2}(\Gamma)$ satisfying $T_1|_\Gamma = g_1$, such that the problem (3.10) has a solution $(\mathbf{u}, T) \in \mathbf{H}_0^1(\Omega) \times H^1(\Omega)$, where $T = T_1 + T_0$ and $T_0 \in H_0^1$. Furthermore, there exist constants C_u and C_H depending only on $\|\mathbf{j}\|_{0,\Omega}$ and the stability constants $\alpha_A, \alpha_C, \alpha_2, \eta_2, C_D$, such that*

$$\|\mathbf{u}\|_{1,\Omega} \leq C_u \|T_1\|_{1,\Omega} \qquad \|T\|_{1,\Omega} \leq C_H \|T_1\|_{1,\Omega} \tag{3.26}$$

Under additional smoothness and smallness assumptions on the solutions, the following uniqueness theorem holds.

Theorem 3.3.3 *Let* $(\mathbf{u}, T) \in [\mathbf{X} \times \mathbf{W}^{1,\infty}]$ *be a solution to problem (3.25), and assume there exists a sufficiently small constant* $0 < M < \min\{\frac{\alpha_A}{C_S C_\infty + K}, \frac{\alpha_C}{L_\alpha + K}\}$*, where* $K = (C_T C_\infty + L_\alpha)/2$*, such that*

$$\max\{\|\mathbf{j}\|_{0,\Omega}, \|\mathbf{u}\|_{\mathbf{W}^{1,\infty}} \|T\|_{W^{1,\infty}}\} < M. \tag{3.27}$$

Then, the solution is unique.

Proof: The proof can be found in [34, Theorem 2.3], which is motivated by a similar argument in [6] for Stokes-Oldroyd problems. ■

3.4 Discrete Problem

To formulate the discontinuous Galerkin method, we first introduce the following discrete spaces

$$\begin{aligned}
\mathbf{V}_h &:= \{\mathbf{v} \in H(\mathrm{div}; \Omega) : \ \mathbf{v}|_{\mathrm{K}} \in \mathbf{RT}_{\mathrm{k}}(\mathrm{K}),\ \forall \mathrm{K} \in \mathcal{T}_{\mathrm{h}},\ \mathbf{v} \cdot \mathbf{n} = 0, \ \text{ on } \Gamma\} \\
Q_h &:= \{q \in L_0^2(\Omega) : \ q|K \in \mathbb{Q}_k(K),\ \forall K \in \mathcal{T}_h\} \\
E_h &:= \{S \in \mathcal{C}^0(\bar{\Omega}) : \ S|_K \in \mathbb{Q}_k(K),\ \forall K \in \mathcal{T}_h;\ S = g_h^T, \text{ on } \Gamma\} \\
E_h^0 &:= \{S \in \mathcal{C}^0(\bar{\Omega}) : \ S|_K \in \mathbb{Q}_k(K),\ \forall K \in \mathcal{T}_h;\ S = 0, \text{ on } \Gamma\} \\
\Lambda_h &:= \{\xi \in C(\bar{\Gamma}) : \ \xi|_e \in \mathbb{Q}_k(e),\ e \in \mathcal{E}_h^B\}
\end{aligned}$$

where $g_h^T \in \Lambda_h$ is the approximate boundary datum which will be defined in Section **??**. We have used the same element pair for the approximation of the velocity and the pressure. And the temperature is approximated with the standard conforming method.

By following the discretization of the viscous term, pressure gradient and the incompressibility constraint in Chapter 1 and by using the standard upwind form in [31] for the nonlinear convection term defined by

$$O_h^N(\mathbf{u}, \mathbf{v}; \mathbf{w}) = \sum_{K \in \mathcal{T}_h} \int_K (\mathbf{w} \cdot \nabla)\mathbf{u} \cdot \mathbf{v}\, d\mathbf{x} + \sum_{K \in \mathcal{T}_h} \int_{\partial K \setminus \partial\Omega} \frac{1}{2}(\mathbf{w} \cdot \mathbf{n}_K - |\mathbf{w} \cdot \mathbf{n}_K|)(\mathbf{u}^e - \mathbf{u}) \cdot \mathbf{v}\, ds$$

and conforming discretization for the convection-diffusion equation (3.10c), we define the DG method as: find $(\mathbf{u}_h, p_h, T_h) \in \mathbf{V}_h \times Q_h \times E_h$, such that

$$A_h(\mathbf{u}_h, \mathbf{v}; T_h) + O_h^N(\mathbf{u}_h, \mathbf{v}; \mathbf{u}_h) + B_h(\mathbf{v}, p_h) - D_h(T_h, \mathbf{v}) = 0 \tag{3.28a}$$

$$-B_h(\mathbf{u}_h, q) = 0 \tag{3.28b}$$

$$C(T_h, S; T_h) + O_H(T_h, S; \mathbf{u}_h) = 0 \tag{3.28c}$$

for all $(\mathbf{v}, q, S) \in \mathbf{V}_h^0 \times Q_h \times E_h^0$, where

$$\begin{aligned} A_h(\mathbf{u}, \mathbf{v}; O) = & \int_\Omega \alpha(O) \nabla_h \mathbf{u} : \nabla_h \mathbf{v} \, d\mathbf{x} - \int_\Omega (\nabla_h \cdot \mathbf{v}) p \, d\mathbf{x} \\ & + \frac{\kappa_0}{h} \int_{\mathcal{E}_h^I} \alpha(T) \underline{[\![\mathbf{u}]\!]} : \underline{[\![\mathbf{v}]\!]} \, ds \\ & - \int_{\mathcal{E}_h^I} \alpha(O) \underline{[\![\mathbf{u}]\!]} : \{\!\{\nabla_h \mathbf{v}\}\!\} \, ds - \int_{\mathcal{E}_h^I} \alpha(O) \underline{[\![\mathbf{v}]\!]} : \{\!\{\nabla_h \mathbf{u}\}\!\} \, ds \\ & + \frac{\kappa_0}{h} \int_{\mathcal{E}_h^B} \alpha(O) \mathbf{u} \cdot \mathbf{v} \, ds \\ & - \int_{\mathcal{E}_h^B} \alpha(O) (\mathbf{u} \otimes \mathbf{n}) : \nabla_h \mathbf{v} \, ds - \int_{\mathcal{E}^B} \alpha(O) (\mathbf{v} \otimes \mathbf{n}) : \nabla_h \mathbf{u} \, ds \end{aligned} \tag{3.29}$$

$$\begin{aligned} O_h^N(\mathbf{u}, \mathbf{v}; \mathbf{w}) = & \sum_{K \in \mathcal{T}_h} \int_K (\mathbf{w} \cdot \nabla) \mathbf{u} \cdot \mathbf{v} \, d\mathbf{x} \\ & + \sum_{K \in \mathcal{T}_h} \int_{\partial K \setminus \partial\Omega} \frac{1}{2} (\mathbf{w} \cdot \mathbf{n}_K - |\mathbf{w} \cdot \mathbf{n}_K|)(\mathbf{u}^e - \mathbf{u}) \cdot \mathbf{v} \, ds \\ & - \int_{\partial\Omega} \frac{1}{2} (\mathbf{w} \cdot \mathbf{n}_K - |\mathbf{w} \cdot \mathbf{n}_K|)(\mathbf{u} \cdot \mathbf{v}) \, ds \end{aligned} \tag{3.30}$$

$$B_h(\mathbf{v}, q) = \int_\Omega (\nabla_h \cdot \mathbf{u}) q \, d\mathbf{x} \tag{3.31}$$

$$D_h(\mathbf{v}, T) = \int_\Omega T \mathbf{j} \cdot \mathbf{v} \, d\mathbf{x} \tag{3.32}$$

$$C(T, S; O) = \int_\Omega \eta(O) \nabla T \cdot \nabla S \, dx \tag{3.33}$$

$$O_H(T, S; \mathbf{w}) = \int_\Omega (\mathbf{w} \cdot \nabla T) S \, dx \tag{3.34}$$

For the boundary datum g_T, we assume

$$g_T \in C(\bar{\Gamma}). \tag{3.35}$$

For continuous function in $C(\bar{\Omega})$, we can define the Larange interpolation operator $\mathcal{I} : C(\bar{\Omega}) \to E_h$. Its restriction to the boundary nodes is denoted by $\mathcal{I}_\Gamma : C(\bar{\Gamma}) \to \Lambda_h$. We take the discrete boundary datum to be $g_h^T = \mathcal{I}_\Gamma g_T$.

Since we have employed the same approximation spaces for the velocity and pressure and the same incompressibility form $B_h(\cdot, \cdot)$ as in Chapter 1, we should expect the exact satisfaction of the incompressibility constraint $\nabla \cdot \mathbf{u}_h \equiv 0$ to be preserved. Actually, we have the following proposition:

Proposition 3.4.1 *The approximate velocity* $\mathbf{u}_h \in \mathbf{V}_h$ *obtained by (3.28) is exactly divergence-free, i.e., it satisfies*

$$\nabla \cdot \mathbf{u}_h \equiv 0 \tag{3.36}$$

Proof: The proof is exactly the same as that of Proposition 3.3 in Chapter 1. ■

As discussed in [13], an important consequence of Proposition 3.4.1 is the provable energy-stability of the numerical method (3.28), without modifying the convective terms in the incompressible Navier-Stokes equation. Moreover, the exact conservation of mass is of great importance in the simulation of the incompressible flow and nearly incompressible materials; see [32] and [4].

3.5 Stability

In this section, we review the stability results in [34, Section 3.3] for the linear forms appearing in the discrete problem (3.28) and adapt them to the $\mathbf{RT}_k - \mathbb{Q}_k$ space pair.

3.5.1 Preliminaries

We restrict the discussion in the broken Sobolev spaces

$$\mathbf{H}^r(\mathcal{T}_h) = \{\mathbf{v} \in \mathbf{L}^2(\Omega) : \mathbf{v}|_K \in \mathbf{H}^r(K),\ K \in \mathcal{T}_h\}, \quad r = 1 \text{ or } 2 \tag{3.37}$$

endowed with the norms

$$\|\mathbf{v}\|_{1,h}^2 = \sum_{K\in\mathcal{T}_h} \|\nabla_h \mathbf{v}\|_{0,K}^2 + \sum_{e\in\mathcal{E}_h} \kappa_0 h_e^{-1} \|\underline{[\![\mathbf{v}]\!]}\|_{0,e}^2, \qquad \mathbf{v} \in \mathbf{H}^1(\mathcal{T}_h) \tag{3.38}$$

$$\|\mathbf{v}\|_{2,h}^2 = \|\mathbf{v}\|_{1,h}^2 + \sum_{K\in\mathcal{T}_h} h_k^2 |\mathbf{v}|_{2,K}^2, \qquad \mathbf{v} \in \mathbf{H}^2(\mathcal{T}_h) \tag{3.39}$$

For $K \in \mathcal{T}_h$, $q \in \mathbb{Q}_k(K)$, by the standard inverse estimate (see e.g. [7, Lemma 4.5.3]), we have $|q|_{2,K} \le Ch^{-1}|q|_{1,K}$. Then it's easy to see that

$$\|\mathbf{v}\|_{2,h} \le C\|\mathbf{v}\|_{1,h}, \ \ \mathbf{v} \in \mathbf{V}_h \tag{3.40}$$

In the analysis of the stability, we need the following embedding result for $d = 2$ (see [20, Lemma 6.2]): For $\mathbf{v} \in \mathbf{H}^1(\mathcal{T}_h)$ and $\forall p \in [1, \infty)$, there exists a constant $C > 0$ such that

$$\|\mathbf{v}\|_{\mathbf{L}^p(\Omega)} \le C\|\mathbf{v}\|_{1,h} \tag{3.41}$$

Moreover, we need the broken $\mathbf{C}^1(\mathcal{T}_h)$-space given by

$$\mathbf{C}^1(\mathcal{T}_h) = \{\mathbf{u} \in H^1(\mathcal{T}_h) : \mathbf{u}|_K \in \mathbf{C}^1(K),\ K \in \mathcal{T}_h\} \tag{3.42}$$

equipped with the broken $\mathbf{W}^{1,\infty}$-norm

$$\|\mathbf{u}\|_{\mathbf{W}^{1,\infty}(\mathcal{T}_h)} = \max_{K\in\mathcal{T}_h} \|\mathbf{u}\|_{\mathbf{W}^{1,\infty}(K)} \tag{3.43}$$

At last, we assume the convective velocity $\mathbf{w} \in \mathbf{H}_0(\mathrm{div}^0, \Omega)$, where the space $\mathbf{H}_0(\mathrm{div}^0, \Omega)$ is defined to be

$$\mathbf{H}_0(\mathrm{div}^0, \Omega) := \{\mathbf{w} \in \mathbf{H}(\mathrm{div}; \Omega) : \ \nabla \cdot \mathbf{w} = 0, \ \mathbf{w} \cdot \mathbf{n} = 0\} \tag{3.44}$$

3.5.2 Continuity

Since we employ conforming elements for the convection-diffusion equation (3.62c), the continuity of $C(T_h, S; \cdot)$ and the Lipschitz continuity of $C(\cdot, \cdot; T)$ are direct consequences of (3.12) and (3.15). For the elliptic form A_h, since we have the $\mathbb{Q}_k(K)$-version trace inequality [37, Lemma 7.1]

$$\|q\|_{0,\gamma_m} \leq C h_K^{-1/2} \|q\|_{0,K}, \quad \forall q \in \mathbb{Q}_k(K). \tag{3.45}$$

as well as the inverse estimate (3.40), we proceed in the standard argument in [3] to obtain the following result.

Lemma 3.5.1 (Boundedness of A_h) *For the form A_h defined in (3.29), there holds*

$$|A_h(\mathbf{u}, \mathbf{v}; \cdot)| \leq C\|\mathbf{u}\|_{2,h}\|\mathbf{v}\|_{1,h}, \qquad \mathbf{u} \in \mathbf{H}^2(\mathcal{T}_h), \ \mathbf{v} \in \mathbf{V}_h, \tag{3.46}$$

$$|A_h(\mathbf{u}, \mathbf{v}; \cdot)| \leq \tilde{C}_A\|\mathbf{u}\|_{1,h}\|\mathbf{v}\|_{1,h}, \qquad \mathbf{u}, \ \mathbf{v} \in \mathbf{V}_h \tag{3.47}$$

The Lipschitz contiuity of $A_h(\cdot, \cdot; T)$ is presented in the next lemma

Lemma 3.5.2 (Lipschitz continuity of A_h) *Let T_1, $T_2 \in H^1(\Omega)$, $\mathbf{u} \in \mathbf{H}_0^1(\Omega)$ and $\mathbf{v} \in \mathbf{V}_h$, then there holds*

$$|A_h(\mathbf{u}, \mathbf{v}; T_1) - A_h(\mathbf{u}, \mathbf{v}; T_2)| \leq L_{A_h} L_\alpha \|T_1 - T_2\|_{1,\Omega}\|\mathbf{u}\|_{1,\infty}(\mathcal{T}_h)\|\mathbf{v}\|_{1,h} \tag{3.48}$$

Proof: The proof can be found in [34, Lemma 3.3].
Moreover, we have the boundedness of B_h and D_h:

Lemma 3.5.3 *We have the following bounds for the forms B_h and D_h.*

$$|B_h(\mathbf{v}, q)| \leq \tilde{C}_B\|\mathbf{v}\|_{1,h}\|q\|_{0,\Omega}, \qquad \mathbf{v} \in \mathbf{H}^1(\mathcal{T}_h), \ q \in L_0^2(\Omega), \tag{3.49}$$

$$|D_h(S, \mathbf{v})| \leq \tilde{C}_D\|\mathbf{j}\|_{0,\Omega}\|S\|_{1,\Omega}\|\mathbf{v}\|_{1,h}, \qquad \mathbf{v} \in \mathbf{H}^1(\mathcal{T}_h), \ S \in H^1(\Omega) \tag{3.50}$$

Proof: Equation (3.49) is a straightforward application of the Cauchy-Schwarz inequality. For the estimate of D_h, by Hölder's inequality and the embedding inequality (3.41), we have

$$|D_h(S,\mathbf{v})| \leq \|\mathbf{j}\|_{0,\Omega}\|S\mathbf{v}\|_{0\Omega} \leq \|\mathbf{j}\|_{0,\Omega}\|S\|_{L^4,\Omega}\|\mathbf{v}\|_{L^4,\Omega} \leq \tilde{C}_D\|\mathbf{j}\|_{0,\Omega}\|S\|_{1,\Omega}\|\mathbf{v}\|_{1,h}$$

■

At last, we review the continuity results for the convection forms O_h^N and O_H.

Lemma 3.5.4 *Let* $\mathbf{w}_1$, $\mathbf{w}_2 \in \mathbf{H}_0(\mathrm{div}^0;\Omega)$, $\mathbf{u} \in \mathbf{H}^2(\Omega)$ *and* $\mathbf{v} \in \mathbf{V}_h$. *Then we have*

$$|O_h^N(\mathbf{u},\mathbf{v};\mathbf{w}_1) - O_h^N(\mathbf{u},\mathbf{v};\mathbf{w}_2)| \leq L_{O_h^N}\|\mathbf{w}_1 - \mathbf{w}_2\|_{1,h}\|\mathbf{u}\|_{1,h}\|\mathbf{v}\|_{1,h} \tag{3.51}$$

Proof: Please refer to [13, Proposition 4.2].

For the conforming convective form $O_H(T,S;\mathbf{w})$, in the case that $\mathbf{w} \in \mathbf{H}_0(\mathrm{div}^0;\Omega)$, we have the following variant of the result in (3.17) .

Lemma 3.5.5 *Let* $\mathbf{w} \in \mathbf{H}_0(\mathrm{div}^0;\Omega)$ *and* $T, S \in H^1(\Omega)$, *we have*

$$|O_H(T,S;\mathbf{w})| \leq \tilde{C}_H\|T\|_{1,\Omega}\|\mathbf{w}\|_{1,h}\|S\|_{1,\Omega} \tag{3.52}$$

Proof: The proof can be found in [34, Lemma 3.5], which involves the application of integration by parts, Hölder's inequality and the embedding result in (3.41). ■

3.5.3 Coercivity and inf-sup condition

In this section we review the coercivity results of the forms A_h, C, O_h^N and O_H as well as the inf-sup condition for B_h.

Lemma 3.5.6 *For* $S \in E_h^0$ *and* $\mathbf{v} \in \mathbf{V}_h$ *we have the following results*

$$C(S,S;\cdot) \geq \alpha_C\|S\|_{1,\Omega} \tag{3.53}$$

$$A_h(\mathbf{v},\mathbf{v};\cdot) \geq \tilde{\alpha}_A\|\mathbf{v}\|_{1,h} \tag{3.54}$$

Proof: Since $E_h^0 \in H_0^1(\Omega)$, the first inequality is a direct consequence of (3.20). By noticing that the perturbed form $\tilde{A}_h = A_h$ when restricted to the discrete space $\mathbf{V}_h$, the second one follows the covercivity result, Proposition 2.4.1 in Chapter 1. ■

For the convective terms O_h^N and O_H we have the following positivity results.

Lemma 3.5.7 *Let* $\mathbf{w} \in \mathbf{H}_0(\mathrm{div}^0;\Omega)$. *Then we have*

$$O_h^N(\mathbf{u},\mathbf{u};\mathbf{w}) = \frac{1}{2}\sum_{e\in\mathcal{E}_h^I}\int_e |\mathbf{w}\cdot\mathbf{n}||\,[\![\mathbf{u}\otimes\mathbf{n}]\!]\,|^2\,ds \geq 0, \qquad \mathbf{u}\in\mathbf{V}_h, \tag{3.55}$$

$$O_H(T,T;\mathbf{w}) = 0, \qquad T\in H^1(\Omega) \tag{3.56}$$

Proof: Since $\mathbf{w}\in\mathbf{H}_0(\mathrm{div}^0;\Omega)$ and if we replace $\mathbf{v}$ with $\mathbf{u}$ in (3.30), we can integrate the cell terms by parts and obtain

$$\begin{aligned}
\sum_{K\in\mathcal{T}_h}\int_K(\mathbf{w}\cdot\nabla)\mathbf{u}\cdot\mathbf{u}\,d\mathbf{x} &= \sum_{K\in\mathcal{T}_h}\int_K \frac{1}{2}\mathbf{w}\cdot\nabla|\mathbf{u}|^2\,d\mathbf{x} = \frac{1}{2}\sum_{K\in\mathcal{T}_h}\int_{\partial K}|\mathbf{u}|^2\mathbf{w}\cdot\mathbf{n}\,ds \\
&= \frac{1}{2}\left(\int_{\mathcal{E}_h^I}\{\!\{|\mathbf{u}|^2\}\!\}\,[\![\mathbf{w}]\!]\;ds + \int_{\mathcal{E}_h}\{\!\{\mathbf{w}\}\!\}\cdot\left[\!\left[|\mathbf{u}|^2\right]\!\right]\;ds\right) \\
&= \frac{1}{2}\int_{\mathcal{E}_h^I}\{\!\{\mathbf{w}\}\!\}\cdot\left[\!\left[|\mathbf{u}|^2\right]\!\right]\;ds \\
&= \frac{1}{2}\int_{\mathcal{E}_h^I}\mathbf{w}\cdot\mathbf{n}_1(|\mathbf{u}_1|^2-|\mathbf{u}_2|^2)\,ds
\end{aligned}$$

Here we have used $\nabla\cdot\mathbf{w}=0$ in Ω, the summation identity, $\mathbf{w}\cdot\mathbf{n}=0$ on Γ and the continuity of $\mathbf{w}\cdot\mathbf{n}$ across the inner edges. And we choose the unit normal vector $\mathbf{n}_1$ on each inner edge such that $\mathbf{w}\cdot\mathbf{n}_1\geq 0$.

Moreover, the other edge terms in the $O_h^N(\mathbf{u},\mathbf{u};\mathbf{w})$ can be rewritten into

$$\sum_{K\in\mathcal{T}_h}\int_{\partial K\setminus\partial\Omega}\frac{1}{2}(\mathbf{w}\cdot\mathbf{n}_K-|\mathbf{w}\cdot\mathbf{n}_K|)(\mathbf{u}^e-\mathbf{u})\cdot\mathbf{u}\,d\mathbf{x} = \sum_{e\in\mathcal{E}_h^I}\int_e(\mathbf{w}\cdot\mathbf{n})(\mathbf{u}^e-\mathbf{u})\cdot\mathbf{u}\,d\mathbf{x}.$$

It is obvious that $\mathbf{w}\cdot\mathbf{n}\leq 0$. Then in order to be consistent with our choice of the normal direction above, we add the subindex as below

$$\begin{aligned}
&\sum_{K\in\mathcal{T}_h}\int_{\partial K\setminus\partial\Omega}\frac{1}{2}(\mathbf{w}\cdot\mathbf{n}_K-|\mathbf{w}\cdot\mathbf{n}_K|)(\mathbf{u}^e-\mathbf{u})\cdot\mathbf{u}\,d\mathbf{x} \\
&= \sum_{e\in\mathcal{E}_h^I}\int_e(\mathbf{w}\cdot\mathbf{n}_2)(\mathbf{u}_1-\mathbf{u}_2)\cdot\mathbf{u}_2\,d\mathbf{x} \\
&= -\int_{\mathcal{E}_h^I}(\mathbf{w}\cdot\mathbf{n}_1)(\mathbf{u}_1\cdot\mathbf{u}_2-|\mathbf{u}_2|^2)\,d\mathbf{x}
\end{aligned}$$

Then we can sum the cell terms and the edge terms together and arrives at

$$\begin{aligned} O_h^N(\mathbf{u},\mathbf{u};\mathbf{w}) &= \frac{1}{2}\int_{\mathcal{E}_h^I} \mathbf{w}\cdot\mathbf{n}_1(|\mathbf{u}_1|^2-|\mathbf{u}_2|^2)\,ds - \int_{\mathcal{E}_h^I}(\mathbf{w}\cdot\mathbf{n}_1)(\mathbf{u}_1\cdot\mathbf{u}_2-|\mathbf{u}_2|^2)\,d\mathbf{x} \\ &= \frac{1}{2}\int_{\mathcal{E}_h^I}(\mathbf{w}\cdot\mathbf{n}_1)|\mathbf{u}_1-\mathbf{u}_2|^2\,ds \\ &= \frac{1}{2}\int_{\mathcal{E}_h^I}|\mathbf{w}\cdot\mathbf{n}|\,|[\![\mathbf{u}\otimes\mathbf{n}]\!]|^2\,ds \geq 0 \end{aligned}$$

The positivity of O_N can be very easily obtained by integration by parts and the properties of the space $\mathbf{H}_0(\mathrm{div}^0;\Omega)$. ■

We end this section with the inf-sup condition of the bilinear form $B(\cdot,\cdot)$:

$$\inf_{q\in Q_h}\sup_{\mathbf{v}\in\mathbf{V}_h\setminus\{\mathbf{0}\}}\frac{B(\mathbf{v},q)}{\|\mathbf{v}\|_{1,h}\|q\|_{0,\Omega}} \geq \beta \tag{3.57}$$

where the inf-sup constant $\beta>0$ is independent of h. This condition is same as the one in Chapter 1. The proof can be found in [37].

3.6 Error Analysis

In this section, we review the *a priori* error estimate for the DG method (3.28). Under suitable smoothness and smallness assumptions, we derive the estimate in a straightforward way without introducing the lifting operators; see [3].

3.6.1 Assumptions

Smoothness assumption:
Let $(\mathbf{u},p,T)$ be the exact solution of (3.7), we assume

$$\begin{aligned} &\text{for } k=1: \quad \mathbf{u}\in C^1(\bar\Omega)\cap H^2(\Omega)^2\cap\mathbf{X}, \quad p\in H^1(\Omega), \quad T\in W^{1,\infty}(\Omega)\cap H^2(\Omega) \\ &\text{for } k=2: \quad \mathbf{u}\in H^{k+1}(\Omega)^2\cap\mathbf{X}, \qquad\quad p\in H^k(\Omega), \quad T\in H^{k+1}(\Omega) \end{aligned} \tag{3.58}$$

Smallness assumption:

$$\max\{\|\mathbf{j}\|_{0,\Omega},\|\mathbf{u}\|_{W^{1,\infty}(\Omega)},\|T\|_{W^{1,\infty}(\Omega)}\}\leq M \tag{3.59}$$

for a sufficiently small number M.

3.6.2 Main result

We are ready to present the error estimate result

Theorem 3.6.1 *Let $(\mathbf{u}, p, T)$ be a solution of (3.7) and $(\mathbf{u}_h, p_h, T_h)$ be the approximate solution to (3.28). Under the smoothness assumption (3.58), smallness assumption (3.59) and the assumption on the boundary datum, we have the following estimate:*

$$\|\mathbf{u} - \mathbf{u}_h\|_{2,h} + \|\theta - \theta_h\|_{1,\Omega} \leq Ch^k(\|\mathbf{u}\|_{k+1,\Omega} + \|T\|_{k+1,\Omega}), \tag{3.60}$$

$$\|p - p_h\|_{0,\Omega} \leq Ch^k(\|p\|_{k,\Omega} + \|\mathbf{u}\|_{k+1,\Omega} + \|T\|_{k+1,\Omega}) \tag{3.61}$$

where $C > 0$ is a generic constant which is independent of h.

Proof: In section 3.5, we have obtained the same set of stability results for our choice of the velocity-pressure element pair as those in [34, Section 5]. We can follow the same line in the proof of [34, Theorem 5.1] and with the standard approximation results to arrive at the conclusion. We omit the details here.

3.7 Fixed-point Iteration

The nonlinear nature of the problem requires us to invoke iterative methods and solve a linearized problem in each iteration. Here we follow [14] and [21] and employ the fixed-point method. We start from a initial guess $\mathbf{T}^0$ and $\mathbf{u}_h^0$ which are the solutions of a Stokes problem and a Laplace problem, respectively. Provided we have obtained the approximate velocity, pressure and temperature $\mathbf{x}_h^n = (\mathbf{u}_h^n, p_h^n, T_h^n)$ from the nth iteration, then the following linearized problem will be solved for $\mathbf{x}_h^{n+1} = (\mathbf{u}_h, p_h, T_h)$

$$A_h(\mathbf{u}_h, \mathbf{v}; T_h^n) + O_h^N(\mathbf{u}_h, \mathbf{v}; \mathbf{u}_h^n) + B_h(\mathbf{v}, p_h) - D_h(T_h^n, \mathbf{v}) = 0 \tag{3.62a}$$

$$-B_h(\mathbf{u}_h, q) = 0 \tag{3.62b}$$

$$C(T_h, S; T_h^n) + O_H(T_h, S; \mathbf{u}_h^n) = 0 \tag{3.62c}$$

for all test functions $(\mathbf{v}, q, S)$, which is a decoupled system consisting of a Oseen equation and a convection-diffusion equation. The iteration is terminated once the difference of the entire coefficient vector coefficients between two consecutive iterates is sufficiently small, i.e.

$$\|\mathbf{coeff}^{n+1} - \mathbf{coeff}^n\|_{l^2} \leq \text{tol} \tag{3.63}$$

where $\|\cdot\|_{l^2}$ is the standard l^2 norm over $\mathbb{R}^{N_{\text{dofs}}}$ and "tol" is the fixed tolerance which is taken to be 10^{-8} in the following experiments.

3.8 Numerical Experiments

In this section we present the numerical results for the coupled system (3.7). The code is developed with the *deal.II* finite element library [5]. Since the goal is to confirm the optimal convergence rates for our method and the exactly divergence-free approximate velocity, we employ the direct linear solver provided by the UMFPACK [16].

3.8.1 Smooth Solution

The computational domain is taken to be

$$\Omega = (-1, 1)^2$$

and is decomposed uniformly into rectangular mesh. At the lth level, the meshsize is $h = 2^{-l}$. The test solution is taken to be

$$\begin{aligned} u_1 &= \sin(y) \\ u_2 &= \sin(x) \\ p &= 1 + \sin(xy) \\ T &= 1 + \cos(xy) \end{aligned}$$

And we take the temperature-dependent parameters to be

$$\alpha(T) = \exp(-T), \quad \eta(T) = \exp(T) \tag{3.64}$$

and the vector $\mathbf{j} = (0, 1)^T$. Appropriate right hand side functions are assigned to balance the equation and discretized in the discrete problem. In the numerical methods, the penalty parameter is chosen as

$$\kappa_0 = (k + 1)^2$$

where k is the approximation order.

Initial Guess

For the fixed-point iteration described in Section 3.7, we take the initial guess to be $\mathbf{x}_h^0 = \mathbf{0}$. In this way, in the first iteration, we actually solve a decoupled Stokes problem and a Laplace problem.

Since the boundary values of $\mathbf{u} = \mathbf{g}^u$ is inhomogeneous, the essential boundary condition $\mathbf{u}_h \cdot \mathbf{n} = \mathbf{g}_h^u \cdot \mathbf{n}$ in $\mathbf{V}_h$ must be enforced strongly in each iteration. To this end, we follow the discussion in Chapter 1 for the enforcement of inhomogeneous boundary conditions for the Stokes problem.

Numerical Results

The numerical results of are presented in Table 3.8.1 and Table 3.8.2 as well as in the convergent plots Figure 3.1, 3.2. The expected optimal convergence rates for the error of the velocity as well as the temperature in the L^2-norm are observed. While for the pressure, just like the results for the Stoke's problem, the convergence order is still between $O(h^k)$ and $O(h^{k+1})$. In Table 3.8.1, the errors for the velocity in the DG norm and for the temperature in the H^1 norm are presented. The convergence order $O(h^k)$ is observed. Moreover, the exactly divergence-free property is verified by evaluating $\|\nabla \cdot \mathbf{u}_h\|_\infty$ over a set of quadrature points. At last, the residual plot for the case of $k = 1$ is presented in Figure 1. We see that the iteration numbers increase moderately as we refine the mesh and the residuals decrease in a linear fashion. For $k > 1$, in our experiment, the same phenomenon is observed.

k	l	$\|e_p\|_0$		$\|e_T\|_0$		$\|e_{\mathbf{u}}\|_0$	
1	1	9.86e-02	-	7.16e-02	-	6.75e-02	-
	2	3.50e-02	1.49	1.92e-02	1.90	2.12e-02	1.67
	3	1.32e-02	1.41	4.96e-03	1.95	5.02e-03	2.08
	4	4.62e-03	1.52	1.25e-03	1.98	1.21e-03	2.06
	5	1.53e-03	1.60	3.14e-04	2.00	3.09e-04	1.97
2	1	1.044e-02	-	6.328e-03	-	1.101e-02	-
	2	1.611e-03	2.70	6.998e-04	3.18	1.306e-03	3.08
	3	2.389e-04	2.75	8.498e-05	3.04	1.600e-04	3.03
	4	3.735e-05	2.68	1.055e-05	3.01	1.975e-05	3.02
3	1	6.910e-04	-	1.520e-04	-	4.713e-04	-
	2	7.407e-05	3.22	1.009e-05	3.91	3.295e-05	3.84
	3	7.033e-06	3.40	6.455e-07	3.97	2.049e-06	4.01
	4	6.318e-07	3.48	4.083e-08	3.98	1.242e-07	4.04
4	1	6.456e-05	-	1.201e-05	-	4.212e-05	-
	2	2.375e-06	4.76	3.402e-07	5.14	1.121e-06	5.23
	3	9.623e-08	4.63	1.057e-08	5.01	3.270e-08	5.10

Table 3.1: Numerical results I: IPDG for the non-isothermal problem (3.7) with fixed-point iteration

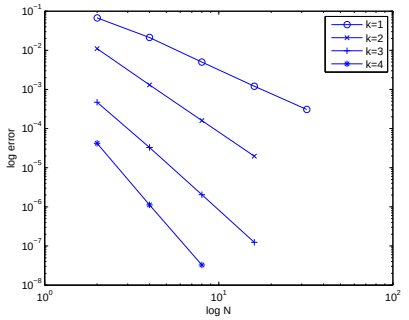

(a) convergent plot for $\|\mathbf{e_u}\|_0$

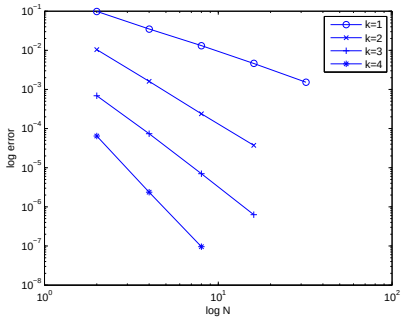

(b) convergent plot for$\|e_p\|_0$

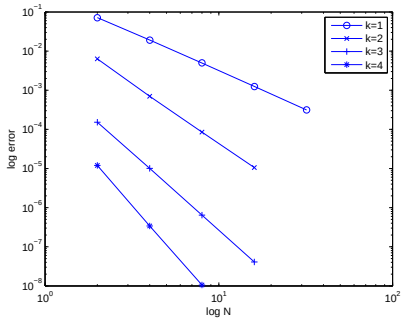

(c) convergent plot for$\|\mathbf{e_T}\|_0$

Figure 3.1: The convergent plots for the numerical errors

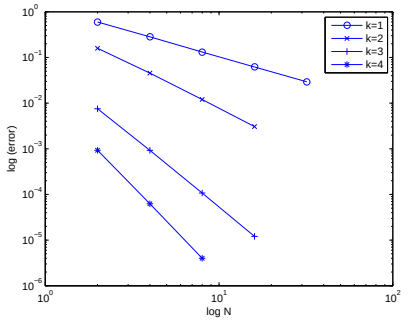

(a) convergent plot for $\|\mathbf{e_u}\|_{1,h}$

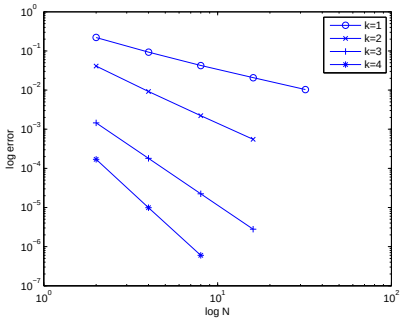

(b) convergent plot for$\|e_T\|_{1,\Omega}$

Figure 3.2: The convergent plots for the numerical errors

k	l	$\|e_{\mathbf{T}}\|_{1,\Omega}$		$\|e_{\mathbf{u}}\|_{1,h}$		$\|\nabla \cdot \mathbf{u}_h\|_\infty$
1	1	2.201e-01	-	5.982e-01	-	1.443e-15
	2	9.332e-02	1.24	2.831e-01	1.08	5.329e-15
	3	4.267e-02	1.13	1.315e-01	1.11	1.199e-14
	4	2.079e-02	1.04	6.195e-02	1.09	2.931e-14
	5	1.030e-02	1.01	2.927e-02	1.08	6.584e-14
2	1	4.108e-02	-	1.591e-01	-	4.732e-15
	2	9.169e-03	2.16	4.546e-02	1.81	1.521e-14
	3	2.223e-03	2.04	1.199e-02	1.92	2.429e-14
	4	5.513e-04	2.01	3.060e-03	1.97	5.556e-14
3	1	1.451e-03	-	7.545e-03	-	1.484e-14
	2	1.805e-04	3.01	9.239e-04	3.03	3.040e-14
	3	2.240e-05	3.01	1.077e-04	3.10	6.105e-14
	4	2.791e-06	3.00	1.206e-05	3.16	1.131e-13
4	1	1.703e-04	-	9.295e-04	-	4.174e-14
	2	9.917e-06	4.10	6.241e-05	3.90	7.412e-14
	3	5.981e-07	4.05	4.010e-06	3.96	1.645e-13

Table 3.2: Numerical results II: IPDG for the non-isothermal problem (3.7) with fixed-point iteration

Figure 3.3: The residual plot for $k = 1$, $l = 1, ..., 4$

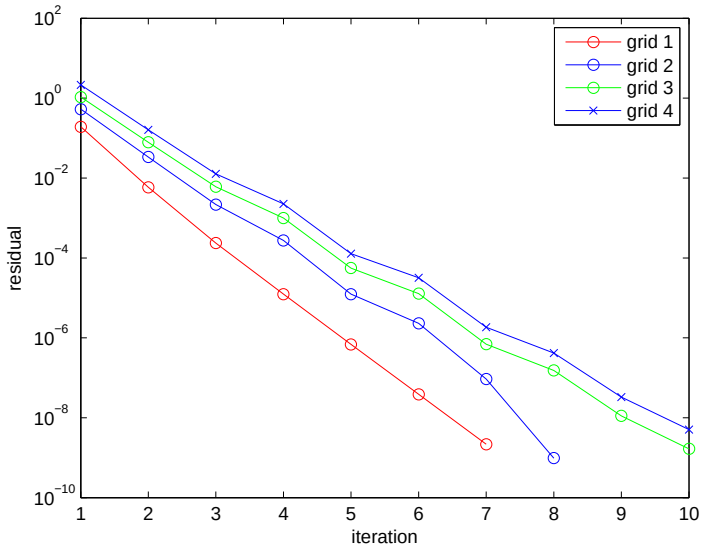

3.9 Conclusions and future directions

In this chapter we first review the formulation and the error analysis in [34] for the exactly divergence-free finite element methods [14], with an $H(\mathrm{div})$ conforming element for the approximate velocity, for a generalised Boussinesq equation [33]. Numerical experiments based on a fixed-point iteration are implemented which verify the theoretical results, especially the error estimates and the exactly divergence-free property. Future work involves:

- More numerical experiments. In this project, only smooth functions in the 2D unit-square domain with Dirichlet boundary conditions is considered. We need to further test the code on singular solutions and more realistic examples in general domains with mixed boundary conditions such as the staircase flows, contraction flows and flows in 3D.

- Efficient nonlinear iteration methods and linear solvers. The first-order fixed point iteration can be replaced with the more efficient Newton's method, while in doing so, the convection term need to be discretized wisely. Even though the direct solvers are super stable, as the mesh is refined or the dimension increased to 3D, the storage requirement for the increasingly large system matrix will be a bottle-neck for the efficiency of the method. Iterative methods need to be considered and efficient preconditioners need to be designed in order to accelerate the convergence.

- More effort in theoretical analysis. As emphasized in [34], the uniqueness of the approximate solution is still a open problem. Even for the existence and the error estimate, very restrictive regularity assumptions (3.58), (3.35) and smallness assumption (3.59) have to be made. It would be another challenge to get rid of these assumptions, while preserving the same optimal error estimates.

Bibliography

[1] D. N. Arnold. An interior penalty finite element method with discontinuous elements. *SIAM J. Numer. Anal.*, 19:742–760, 1982.

[2] D. N. Arnold, F. Brezzi, and M. Fortin. A stable finite element for the Stokes equations. *Calcolo*, 21:337–344, 1984.

[3] Douglas N. Arnold, Franco Brezzi, Bernardo Cockburn, and L. Donatella Marini. Unified analysis of discontinuous Galerkin methods for elliptic problems. *SIAM J. Numer. Anal.*, 39(5):1749–1779, 2002.

[4] F. Auricchio, L. Beirao Da Veiga, C. Lovadina, and A. Reali. The importance of the exact satisfaction of the incompressibility constraint in nonlinear elasticity: mixed FEMs verses NURBS-based approximations. *Comp. Math. Appl. Mech. and Eng.*, 199:314–323, 2010.

[5] W. Bangerth and G. Kanschat. Concepts for object-oriented finite element software-the deal.II library. *Preprint 43, SFB 359*, 1999.

[6] J. Baranger and D. Sandri. A formulation of the Stoke's problem and the linear elasticity equations suggested by the Oldroyd model for viscoelastic flow. *Mathematical Modelling and Numerical Analysis*, 1:331–345, 1992.

[7] S. C. Brenner and L. R. Scott. *The Mathematical Theory of Finite Element Methods*. Springer, 2002.

[8] F. Brezzi and M. Fortin. *Mixed and Hybrid Finite Element Methods*. Springer Verlag, 1991.

[9] A. Buffa, C.de Falco, and G. Sangalli. IsoGeometric analysis: Stable elements for the 2D Stokes equation. *International Journal for Numerical Methods in Fluids*, 65: 1407–1422, 2011.

[10] A. E. Caola, Y. Joo, and R. C. Armstrong. Highly parallel time integration of viscoelastic flows. *Journal of Non-Newtonian Fluid Mechanics*, 100:191–216, 2001.

[11] P. G. Ciarlet. *The Finite Element Methods for Elliptic Problems.* NORTH-HOLLAND, 1978.

[12] P. G. Ciarlet. *Mathematics Elasticity.* NORTH-HOLLAND, 1988.

[13] B. Cockburn, G. Kanschat, and D. Schötzau. A locally conservative LDG method for the incompressible Navier-Stokes equations. *Math. Comp.*, 74:1067–1095, 2005.

[14] B. Cockburn, G. Kanschat, and D. Schötzau. A note on discontinuous Galerkin divergence-free solutions of the Navier-Stokes equations. *Journal of Scientific Computing*, 31:61–73, 2007.

[15] C. Cox, H. Lee, and D. Szurley. Finite element approximation of the non-isothermal Stokes-Oldroyd equations. *International Journal of Numerical Analysis and Modelling*, 1:1–18, 2007.

[16] T. A. Davis. Algorithm 832: UMFPACK V4.3—an unsymmetric-pattern multifrontal method. *ACM Transactions on Mathematical Software*, 30:196–199, 2004.

[17] C. e. P., J. Thomas, S. Blancher, and R. Creff. The steady Navier-Stokes/energy system with temperature-dependent viscosity-Part 1: Analysis of the continuous problem. *International Journal for Numerical Methods in Fluids*, 56:63–89, 2008.

[18] C. e. Pérez, J. Thomas, S. Blancher, and R. Creff. The steady Navier-Stokes/energy system with temperature-dependent viscosity-Part 2: The discrete problem and numerical experiments. *International Journal for Numerical Methods in Fluids*, 56: 91–114, 2008.

[19] M. Farhloul and A. Zine. A dual mixed formulation for non-isothermal Oldroyd-Stokes problem. *Mathematical Modelling of Natural Phenomena*, 6 (05):130–156, 2011.

[20] V. Girault and P. A. Raviart. *Finite element methods for Navier-Stokes equations.* Springer, New York, 1986.

[21] C. Greif, D. Li, D. Schötzau, and X. Wei. A mixed finite element method with exactly divergence-free velocities for incompressible magnetohydrodynamics. *Computer Methods in Applied Mechanics and Engineering*, 199:2840–2855, 2010.

[22] J. Guzmán and M. Neilan. Conforming and divergence free Stokes elements on general triangular meshes. *Mathematics of Computation*, 2011.

[23] J. Guzmán and M. Neilan. Conforming and divergence-free Stokes elements in three dimensions . *IMA Journal of Numerical Analysis*, 2013.

[24] P. Hood and C. Taylor. Numerical solution of the Navier-Stokes equations using the finite element technique. *Compt. Fluids*, 1:1–28, 1973.

[25] J. E. House. *Principles of Chemical Kinetics*. Academic Press, Elsevier, 2004.

[26] Y. Joo, J. Sun, M. Smith, R. Armstrong, R. Brown, and R. Ross. Two-dimensional numerical analysis of non-isothermal melt spinning with and without phase transition. *Journal of Non-Newtonian Fluid Mechanics*, 102:37–70, 2002.

[27] R. E. Khayat and M. O. Starzewski. On the objective rate of heat and stress fluxes. Connection with micro/nano-scale heat convection. *Discrete and Continuous Dynamical Systems-Series B*, 15 (04):991–998, 2011.

[28] L. Kovasznay. Laminar flow behind a two-dimensional grid. *Proc. Camb. Philos. Soc*, 44:58–62, 1948.

[29] M. Kronbichler, T. Heister, and W. Bangerth. High accuracy mantle convection simulation through modern numerical methods. *Geophys. J. Int.*, 191:12–29, 2012.

[30] K. Kunisch and X. Marduel. Optimal control of non-isothermal viscoelastic fluid flow. *Journal of Non-Newtonian Fluid Mechanics*, 88:261–301, 2000.

[31] P. LeSaint and P. A. Raviart. On a finite element method for solving the neutron transport equation. 1974.

[32] A. Linke. Collision in a cross-shaped domain A steady 2D Navier-Stokes example demonstrating the importance of mass conservation in CFD. *Comp. Math. Appl. Mech. and Eng.*, 198:3278–3286, 2009.

[33] S. A. Lorca and J. L. Boldrini. Stationary solutions for generalized boussinesq models. *Journal of Differential Equations*, 124:389–406, 1996.

[34] R. Oyarzúa, T. Qin, and D. Schötzau. An exactly divergence-free finite element method for a generalized Boussinesq problem. *IMA Journal of Applied Mathematics*, accepted.

[35] G. W. M. Peters and F. T. O. Baaijens. Modelling of non-isothermal viscoelastic flow. *Journal of Non-Newtonian Fluid Mechanics*, 68:205–254, 1997.

[36] D. A. D. Pietro and A. Ern. *Mathematical Aspects of the Discontinuous Galerkin Methods*. Springer, 2012.

[37] D. Schötzau, C. Schwab, and A. Toselli. hp-DGFEM for incompressible flows. *SIAM J. Numer. Anal.*, 40:561–571, 2003.

[38] G. Schubert, D. L. Turcotte, and P. Olson. *Mantle Convection in the Earth and Planets, Part 1.* Cambridge University Press, Cambridge, 2001.

[39] L. R. Scott and M. Vogelius. Conforming finite element methods for incompressible and nearly incompressible continua. *Lectures in Applied Mathematics*, 22:221–244, 1985.

[40] R. Témam. Sur l'approximation des solutions des équations de Navier-Stokes. *C. R. Acad. Sci. Paris Sér.*, A 216:219–221, 1966.

[41] R. Témam. Une méthode d'approximation des solutions de la solutions des équations de Navier-Stokes. *Bull. Soc. Math. France*, 98:115–152, 1968.

[42] S. Zhang. Some divergence-free finite elements for the stationary Stokes equations. In Y. Y. Li, C. W. Shu, R. G. Ye, and K. Zuo, editors, *Advances in Mathematics and Its Applications*, pages 261–282. the University of Science and Technology of China Press, Hefei, 2008.